

227th ACS National Meeting, March 28-April 1, 2004 Anaheim, CA

Matching-Pursuit Representations for Simulations of Quantum Processes

Yinghua Wu and Victor S. Batista
Department of Chemistry, Yale University



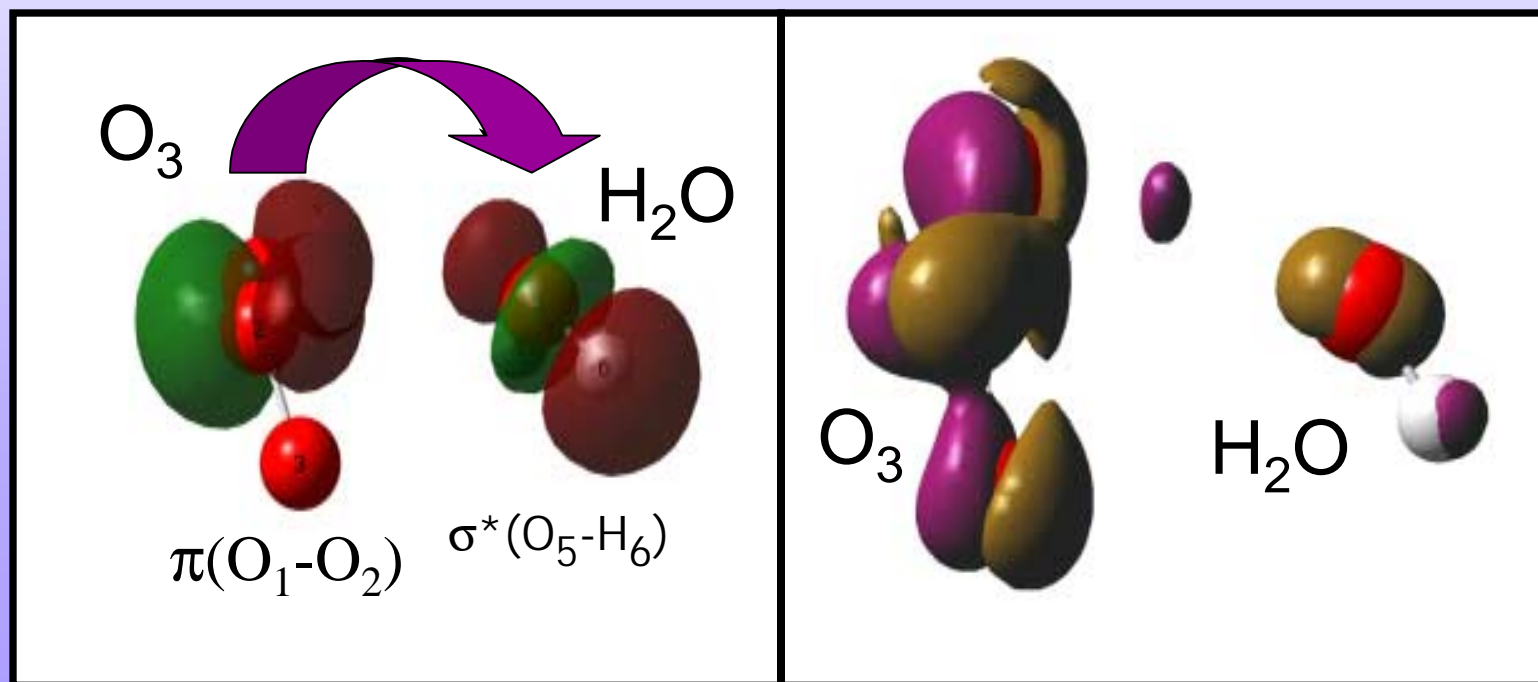
Mr. Yinghua Wu



OZONE-WATER CLUSTERS: NBO ANALYSIS OF STEREOELECTRONIC INTERACTIONS (PHYS 391)

Eduardo M. Sproviero, Devon Philip, Sergio D. Dalosto, and Victor S. Batista

Yale University, *Department of Chemistry, P. O. Box 208107, New Haven Connecticut 06520-8107 USA*





**QM/MM Studies of Protein Polarization due to
Proton Transfer in GFP** **(COMP 197)**

Jose A. Gascon, Siegfried Leung, and Victor S. Batista

**Yale University, *Department of Chemistry, P. O. Box 208107, New Haven
Connecticut 06520-8107 USA***



**Influence of Bound Water Molecules in hydroxylation
and epoxydation reactions in cytochrome P450cam
wild type and T252A mutant** **(PHYS 465)**

Sergio Dalosto, Eduardo M. Sproviero and Victor S. Batista

**Yale University, *Department of Chemistry, P. O. Box 208107, New Haven
Connecticut 06520-8107 USA***

Coherent-Control of Excited State Intramolecular Proton Transfer in 2-(2'-hydroxyphenyl)-oxazole

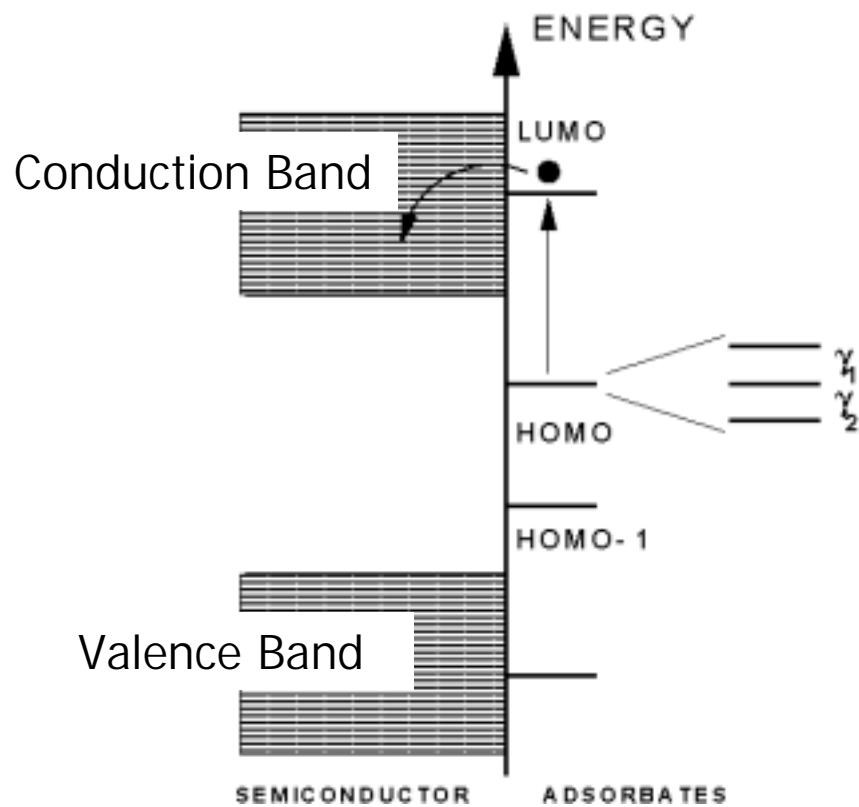
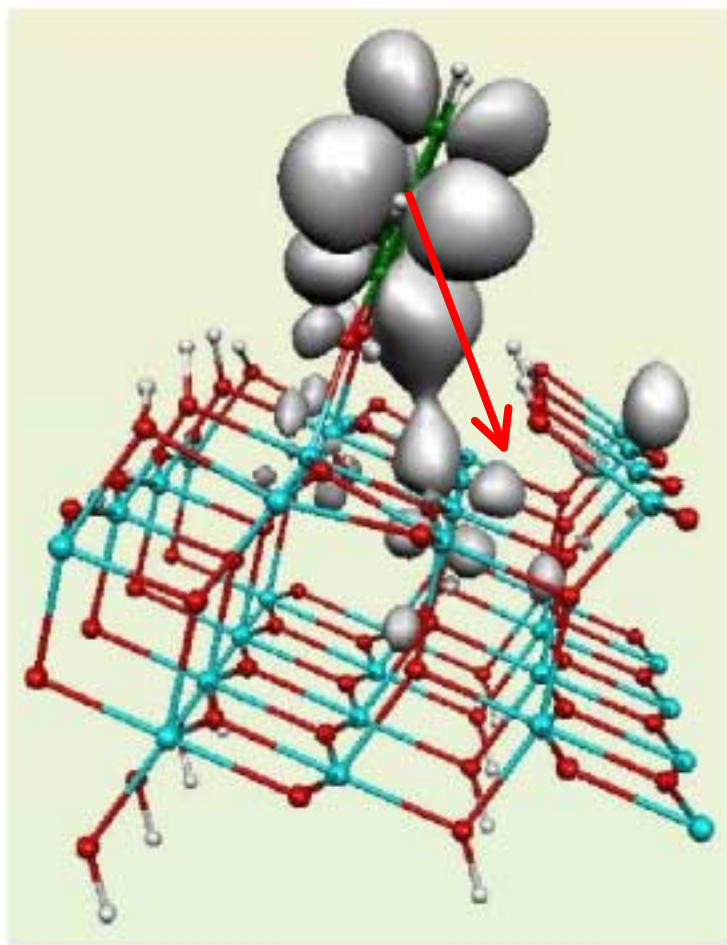
Victor S. Batista and Paul Brumer *Phys. Rev. Lett.* **89**,5889 (2003);
ibid. **89**,28089 (2003)

Model Study of Coherent-Control of Rhodopsin Photoisomerization: The Primary Step in Vision

Samuel Flores and Victor S. Batista *Phys. Chem. B* (in press) (2004)

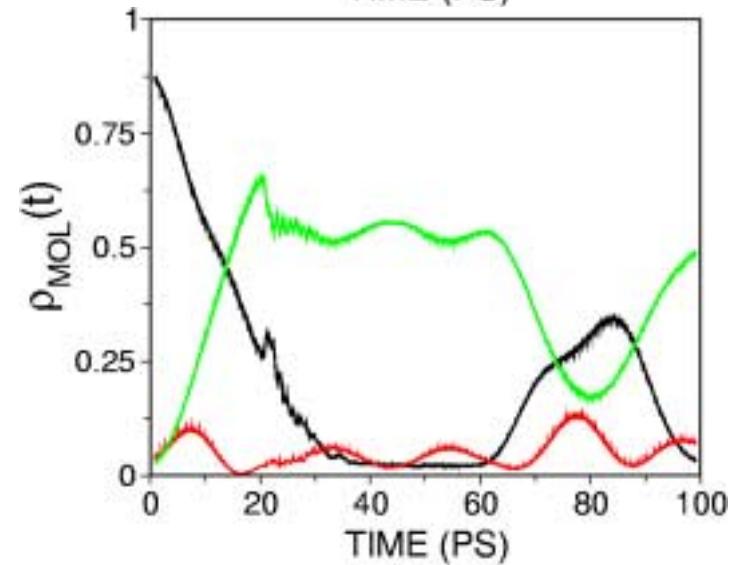
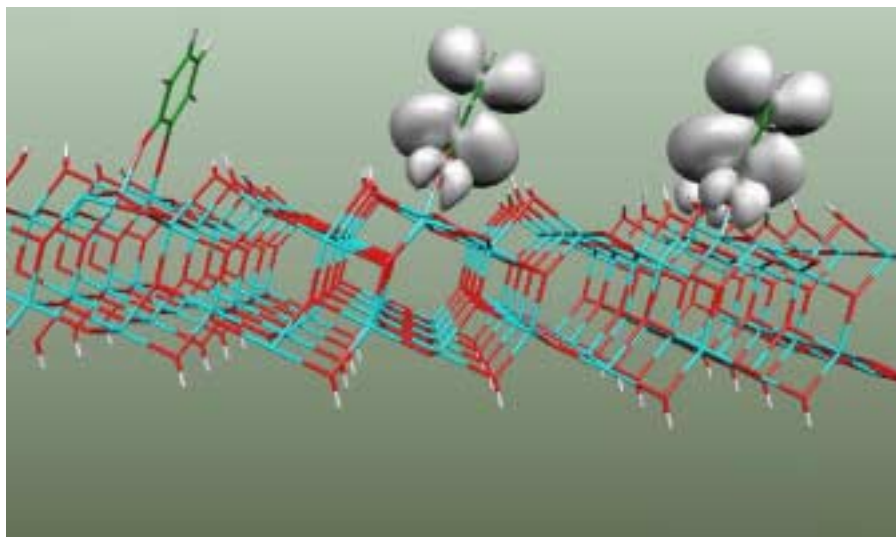
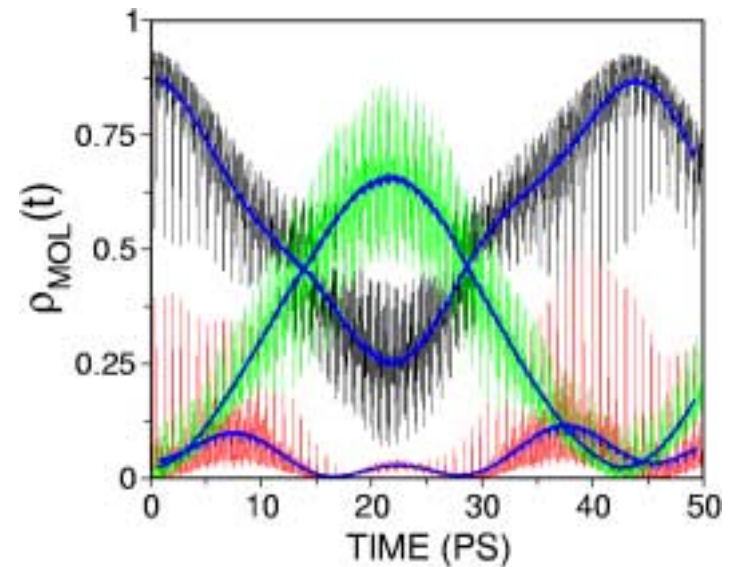
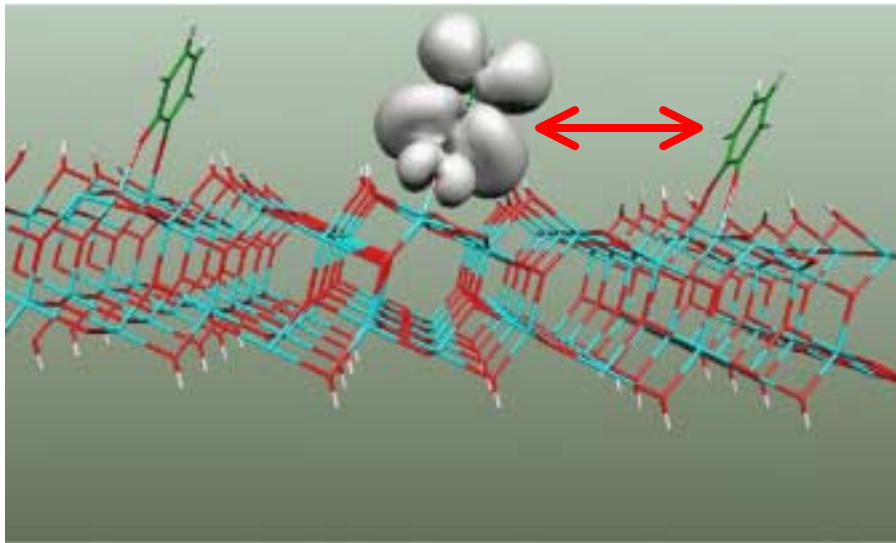
Interfacial Electron Transfer in Functionalized Semiconductors

Luis G.C. Rego and Victor S. Batista *J. Am. Chem. Soc.* **125**,7989 (2003)



Quantum-Entanglement and Coherent-Control of Hole Relaxation Dynamics Localized Deep in the Semiconductor Band Gap

Luis G.C. Rego and Victor S. Batista (*submitted to Phys. Rev. Lett.*)



Time-Sliced Simulations of Quantum Processes

$$\langle \mathbf{x} | \Psi_t \rangle = \int d\mathbf{x}_0 \langle \mathbf{x} | e^{-i\hat{H}(t_n - t_0)/\hbar} | \mathbf{x}_0 \rangle \langle \mathbf{x}_0 | \Psi_0 \rangle,$$

The essence of the approach is to time-slice matrix elements of the quantum mechanical propagator by repeatedly inserting the resolution of identity

$$\hat{1} = \int d\mathbf{x} |\mathbf{x}\rangle \langle \mathbf{x}|,$$

yielding

$$\langle \mathbf{x}_n | e^{-i\hat{H}(t_n - t_0)/\hbar} | \mathbf{x}_0 \rangle = \int d\mathbf{x}_{n-1} \dots \int d\mathbf{x}_1 \langle \mathbf{x}_n | e^{-(i/\hbar)\hat{H}(t_n - t_{n-1})} | \mathbf{x}_{n-1} \rangle \dots \langle \mathbf{x}_1 | e^{-(i/\hbar)\hat{H}(t_1 - t_0)} | \mathbf{x}_0 \rangle,$$

where $t_0 < t_1 < \dots < t_{n-1} < t_n$. For sufficiently thin time slices (i.e., when $\tau = t_k - t_{k-1}$ is sufficiently small) each finite-time propagator can be approximated by a semiclassical (*e.g.*, HK SC-IVR) or a quantum-mechanical expansion (*e.g.*, Trotter expansion).

MP/SOFT Method (Trotter Expansion)

Wu, Y. and Batista, V.S. *J. Chem. Phys.* **118**, 6720 (2003);
ibid. **118**, 6720 (2003); *ibid.* **submitted** (2004).

$$e^{-(i/\hbar)\hat{H}\tau} \approx e^{-(i/\hbar)\hat{V}\tau/2} \text{FT}^{-1} e^{-(i/\hbar)\frac{\hat{\mathbf{p}}^2}{2m}\tau} \text{FT} e^{-(i/\hbar)\hat{V}\tau/2}.$$

Here, $\hat{H} = \frac{\hat{\mathbf{p}}^2}{2m} + \hat{V}(\mathbf{x})$, and FT indicates the action of the multidimensional Fourier transform.

Analytically Continued MP/SOFT Method

- **Step [1]:** Decompose $\langle \mathbf{x} | \tilde{\Psi}_t \rangle \equiv \langle \mathbf{x} | e^{-\frac{i}{\hbar} \hat{V}(\mathbf{x}) \frac{dt}{2}} | \Psi_t \rangle$ in a matching-pursuit coherent-state expansion:

$$\langle \mathbf{x} | \tilde{\Psi}_t \rangle \approx \sum_{j=1}^n c_j \langle \mathbf{x} | j \rangle,$$

where

$$c_j \equiv \begin{cases} \langle 1 | \tilde{\Psi}_t \rangle, & \text{when } j = 1, \\ \langle j | \tilde{\Psi}_t \rangle - \sum_{k=1}^{j-1} c_k \langle j | k \rangle, & \text{otherwise.} \end{cases}$$

Here, $\langle \mathbf{x} | j \rangle$ are N-dimensional coherent-states,

$$\langle \mathbf{x} | j \rangle \equiv \prod_{k=1}^N A_j(k) e^{-\gamma_j(k)(x(k)-x_j(k))^2/2} e^{i p_j(k)(x(k)-x_j(k))}$$

with complex-valued coordinates $x_j(k) \equiv c_j(k) + i d_j(k)$, momenta $p_j(k) \equiv g_j(k) + i f_j(k)$, and scaling parameters $\gamma_j(k) \equiv a_j(k) + i b_j(k)$. The normalization constants are $A_j(k) \equiv (a_j(k)/\pi)^{1/4} \exp[-\frac{1}{2} a_j(k) d_j(k)^2 - d_j(k) g_j(k) - (b_j(k) d_j(k) + f_j(k))^2 / (2 a_j(k))]$.

Matching-Pursuit Coherent-State Expansion

- **Step [1.1]:** Maximize the norm of the overlap of a trial coherent-state with the target state $|\langle j|\tilde{\Psi}_t\rangle|$. Define $|1\rangle$ according to the optimum parameters and the expansion coefficient c_1 as the overlap. Therefore,

$$|\tilde{\Psi}_t\rangle = c_1|1\rangle + |\varepsilon_1\rangle, \quad (-5)$$

- **Step [1.2]:** Goto [1.1], replacing $|\tilde{\Psi}_t\rangle$ by $|\varepsilon_1\rangle$. Therefore,

$$|\varepsilon_1\rangle = c_2|2\rangle + |\varepsilon_2\rangle, \quad (-5)$$

where $c_2 \equiv \langle 2|\varepsilon_1\rangle$.

After n successive orthogonal projections, the norm of the residual vector $|\varepsilon_n\rangle$ is smaller than a desired precision ϵ ,

$$|\varepsilon_n| = \sqrt{1 - \sum_{j=1}^n |c_j|^2} < \epsilon. \quad (-5)$$

Norm conservation is maintained within a desired precision.

- **Step [2]:** Analytically Fourier transform the coherent-state expansion to the momentum representation, apply the kinetic energy part of the Trotter expansion $e^{-\frac{i}{\hbar} \frac{\mathbf{p}^2}{2m} \tau}$, and analytically inverse Fourier transform the resulting expression back to the coordinate representation to obtain the time evolved wavefunction:

$$\langle \mathbf{x} | \Psi_{t+\tau} \rangle = \sum_{j=1}^n c_j e^{-\frac{i}{\hbar} V(\mathbf{x}) \frac{dt}{2}} \langle \mathbf{x} | \tilde{j} \rangle,$$

where

$$\langle \mathbf{x} | \tilde{j} \rangle \equiv \prod_{k=1}^N A_j(k) \sqrt{\frac{m}{m + i\tau\hbar\gamma(k)}} \times \exp \left(\frac{\left(\frac{p_j(k)}{\hbar\gamma(k)} - i(x_j(k) - x(k)) \right)^2}{\left(\frac{2}{\gamma(k)} + \frac{i2\tau\hbar}{m} \right)} - \frac{p_j(k)^2}{2\gamma(k)\hbar^2} \right).$$

Equilibrium Density Matrix

$$\langle \mathbf{x} | \hat{\rho}_\beta | \mathbf{x}_0 \rangle = \langle \mathbf{x} | e^{-\beta \hat{H}} | \mathbf{x}_0 \rangle$$

$$\langle \mathbf{x} | \hat{\rho}_\beta | \mathbf{x}_0 \rangle = \int d\mathbf{x}_{n-1} \dots \int d\mathbf{x}_2 \langle \mathbf{x} | e^{-(\beta_n - \beta_{n-1}) \hat{H}} | \mathbf{x}_{n-1} \rangle \dots \langle \mathbf{x}_2 | e^{-(\beta_2 - \beta_1) \hat{H}} | \mathbf{x}_1 \rangle \langle \mathbf{x}_1 | \rho_\epsilon | \mathbf{x}_0 \rangle,$$

where $\beta = \beta_n - \beta_0$ and $\epsilon = \beta_1 - \beta_0$

$$\langle \mathbf{x}_1 | \rho_\epsilon | \mathbf{x}_0 \rangle = \sqrt{\frac{m}{2\pi\hbar^2\epsilon}} e^{-\epsilon V(\mathbf{x}_0)/2} e^{-\frac{m}{2\hbar^2\epsilon}(\mathbf{x}_1 - \mathbf{x}_0)^2} e^{-\epsilon V(\mathbf{x}_1)/2}$$

$$Z = \int d\mathbf{x}_0 \langle \mathbf{x}_0 | \hat{\rho}_\beta | \mathbf{x}_0 \rangle$$

$$\langle A \rangle = Z^{-1} \int d\mathbf{x}_0 \int d\mathbf{x} \langle \mathbf{x} | \hat{\rho}_\beta | \mathbf{x}_0 \rangle \langle \mathbf{x}_0 | \hat{A} | \mathbf{x} \rangle$$

Electron Tunneling in Multidimensional Systems

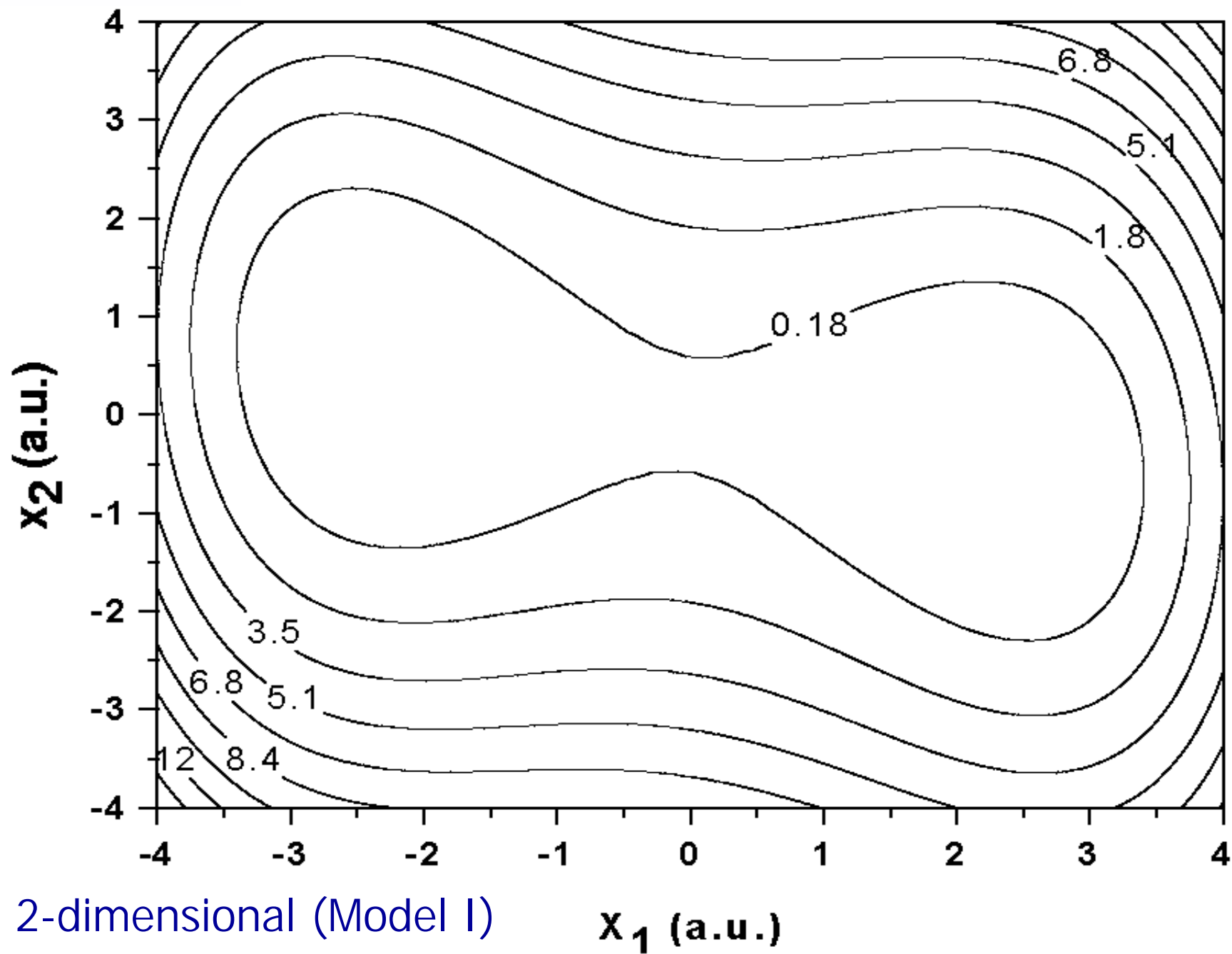
Model I:

$$\hat{H} = \frac{\hat{p}_1^2}{2m_1} + V_1(\hat{x}_1) + \sum_{j=2}^N \left(\frac{\hat{p}_j^2}{2m_j} + \frac{1}{2}m_j\omega_j^2\hat{x}_j^2 + c_j\hat{x}_j\hat{x}_{j-1} \right)$$

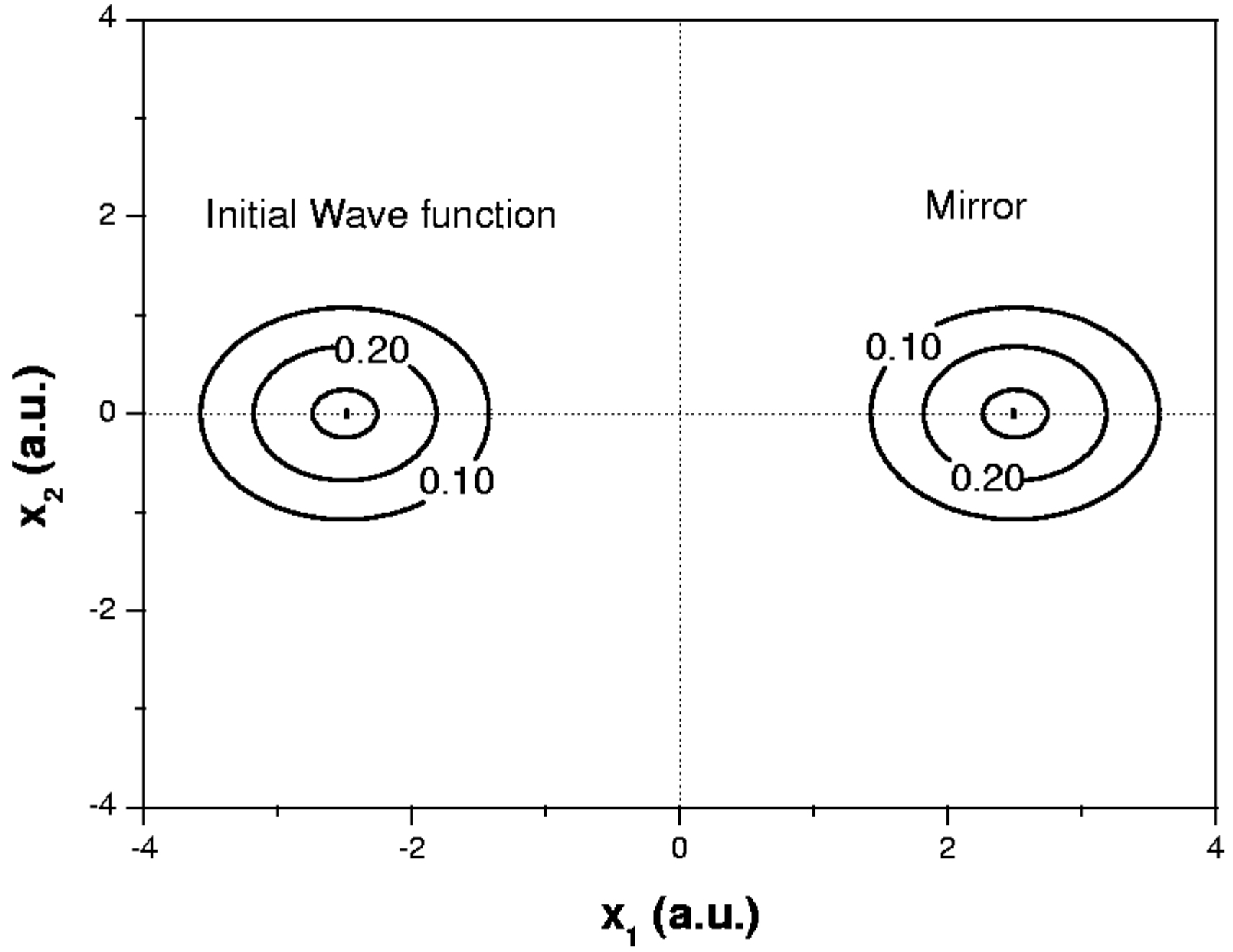
where $m_j = 1.0$ a.u., $\omega_j = 1.0$ a.u. and $c_j = 0.2$ a.u. for $j = 1-N$, with $N = 1-10$

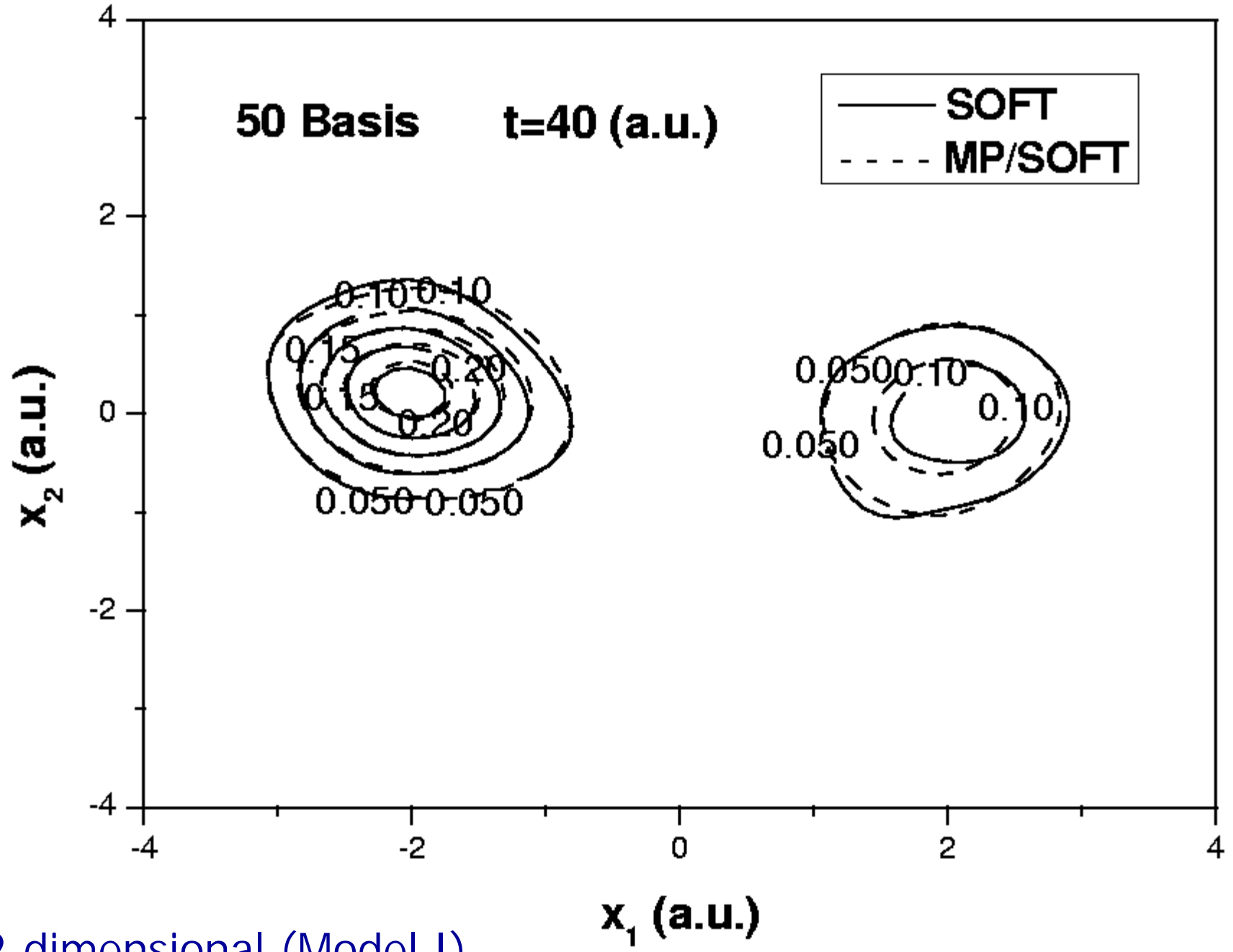
$$V_1(\hat{x}_1) = \frac{1}{16\eta}\hat{x}_1^4 - \frac{1}{2}\hat{x}_1^2,$$

with $\eta = 1.3544$.

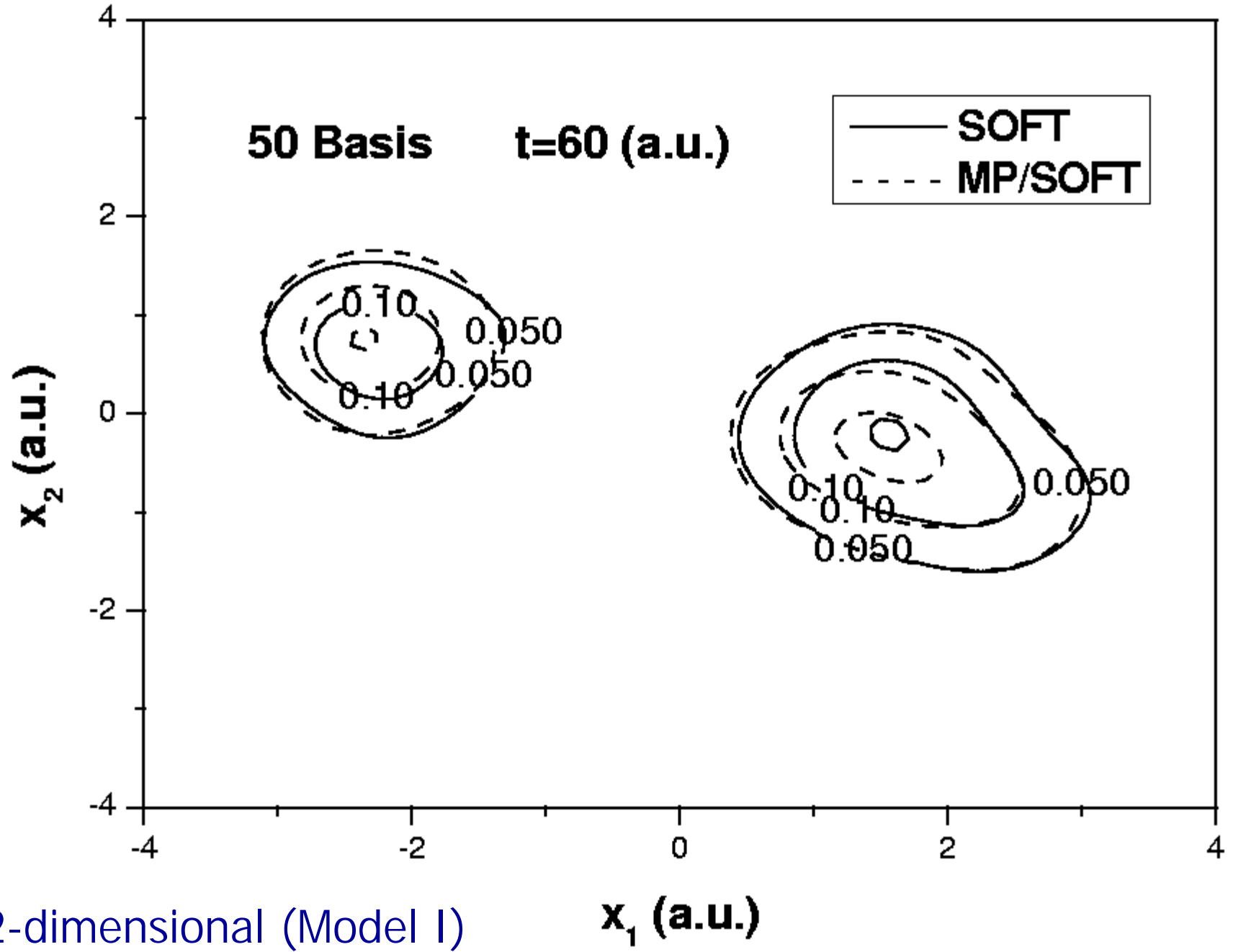


2-dimensional (Model I)

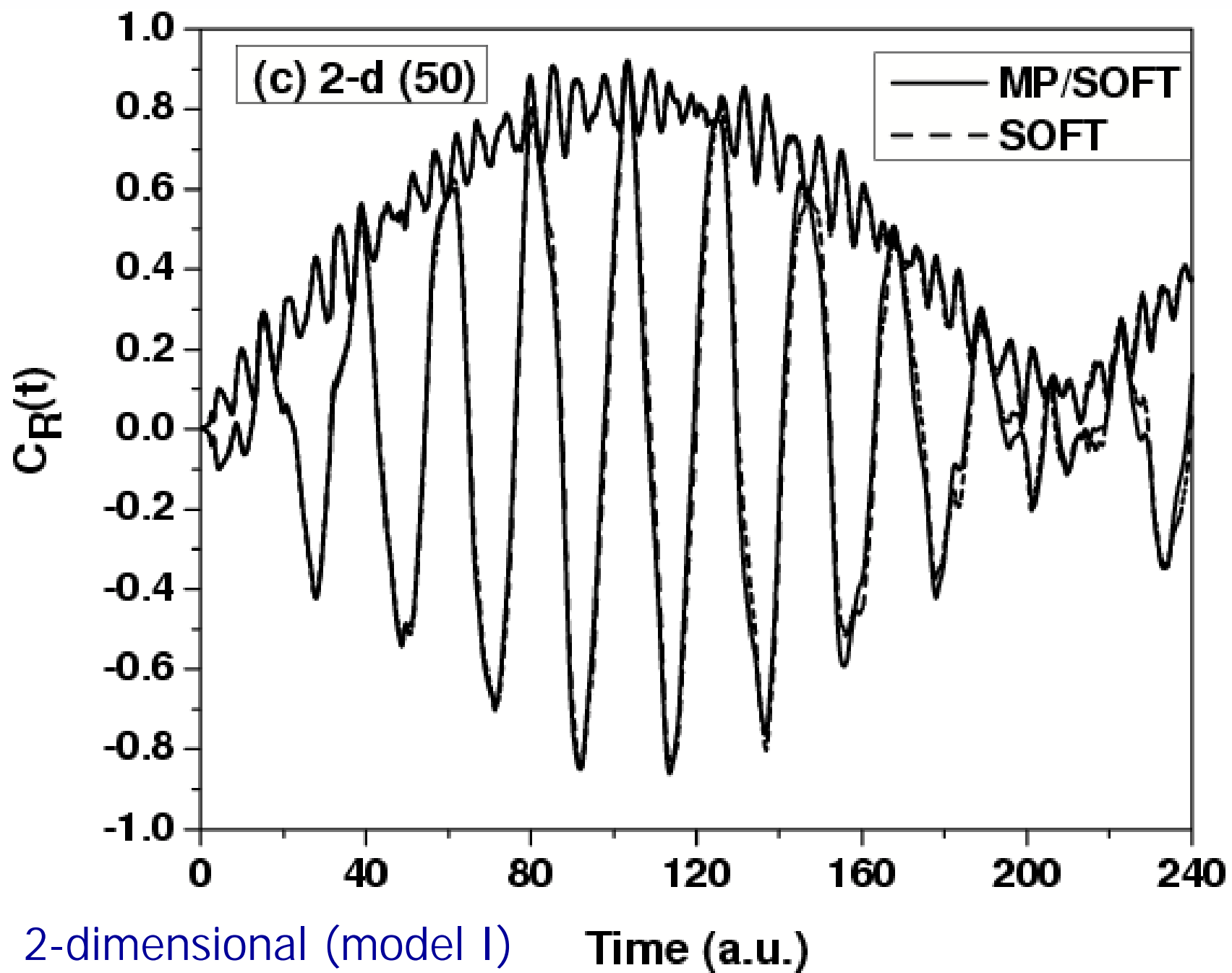


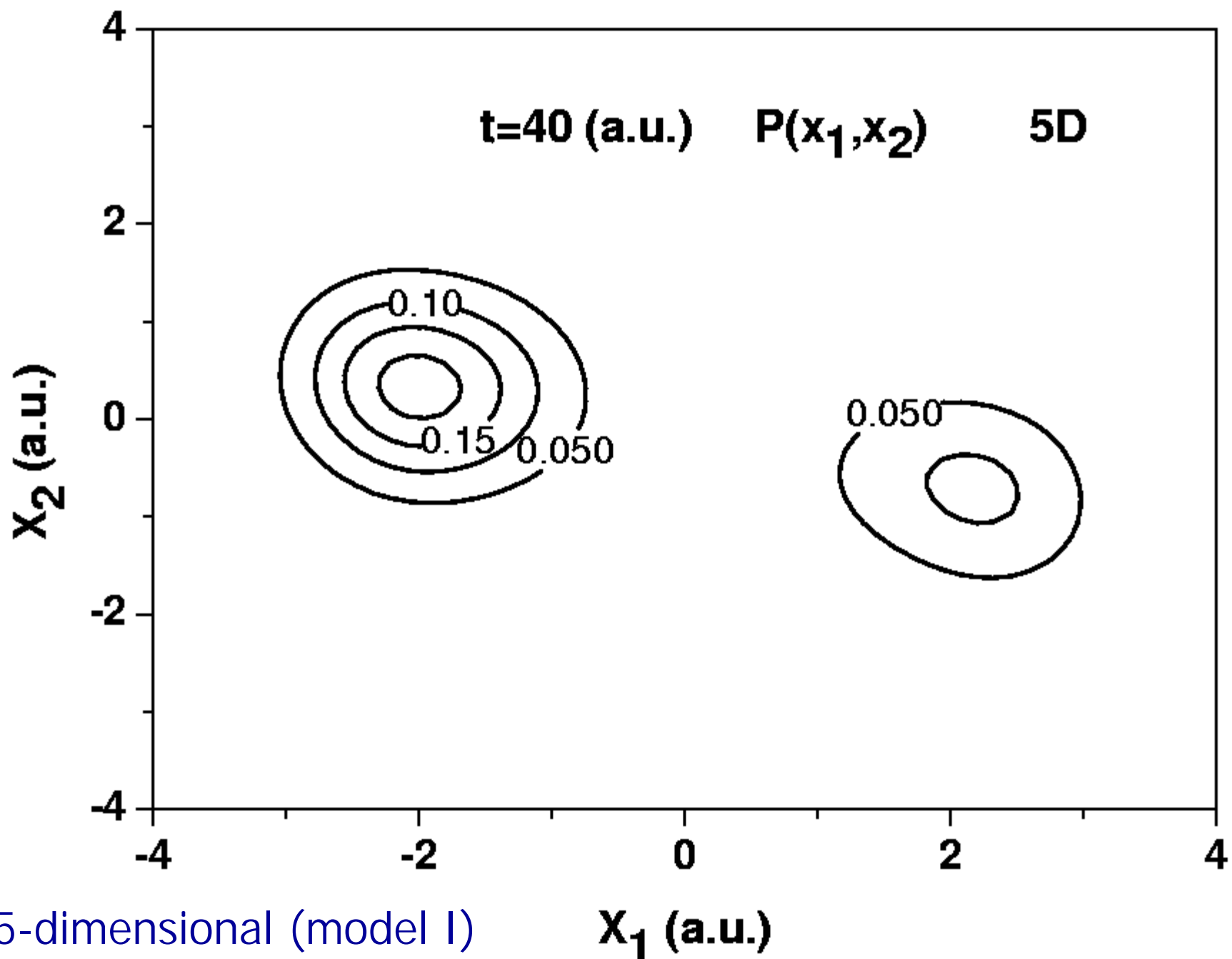


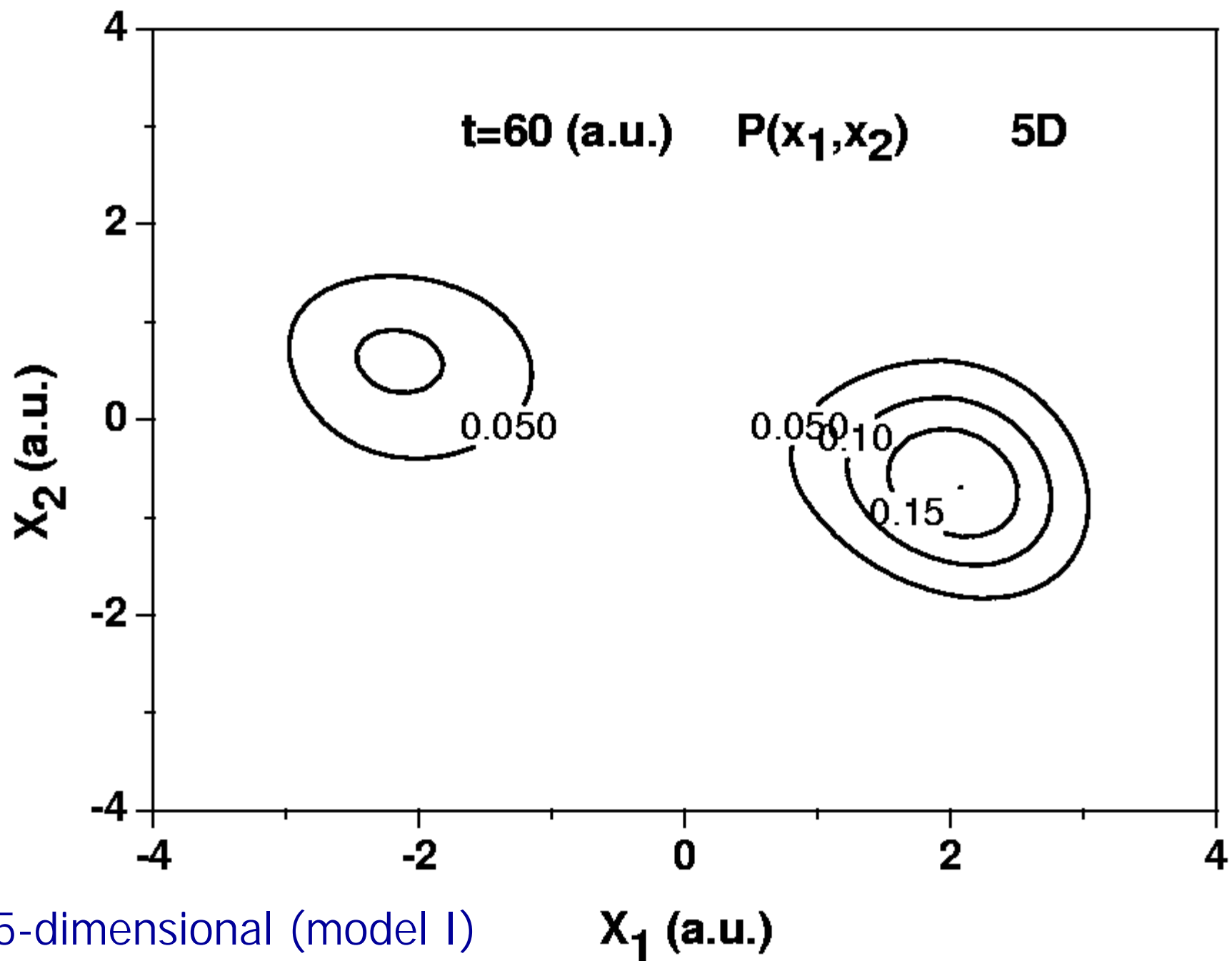
2-dimensional (Model I)

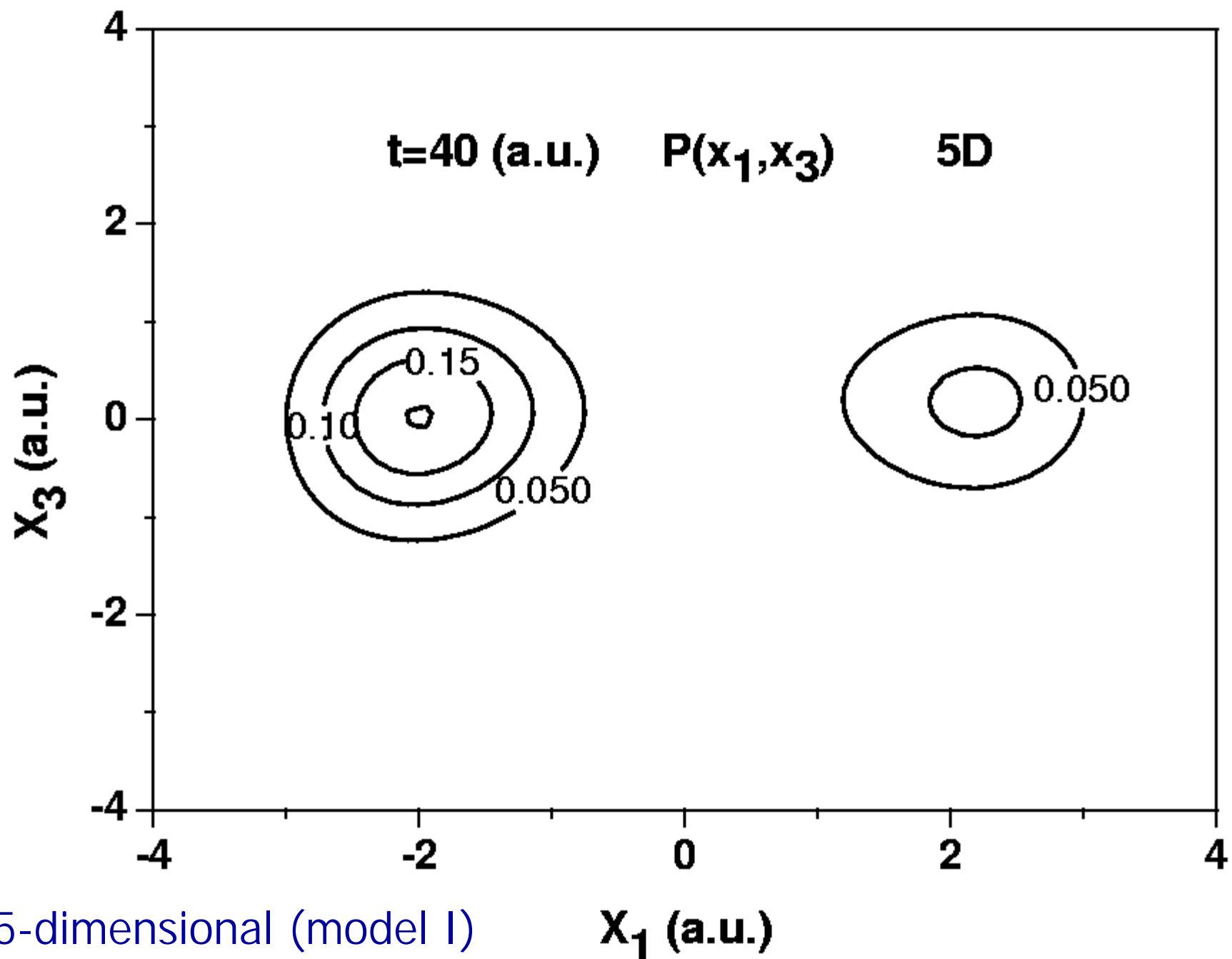


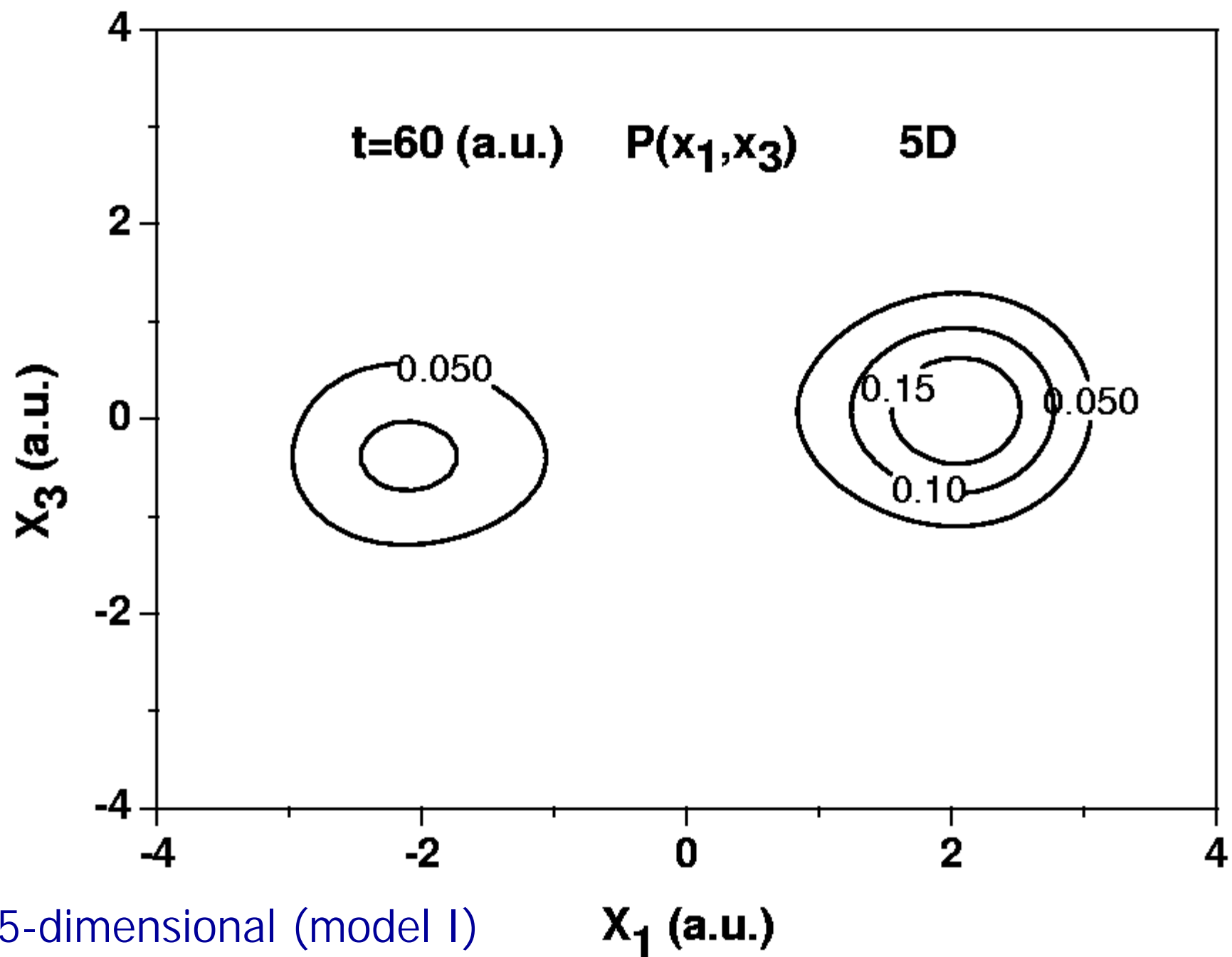
2-dimensional (Model I)

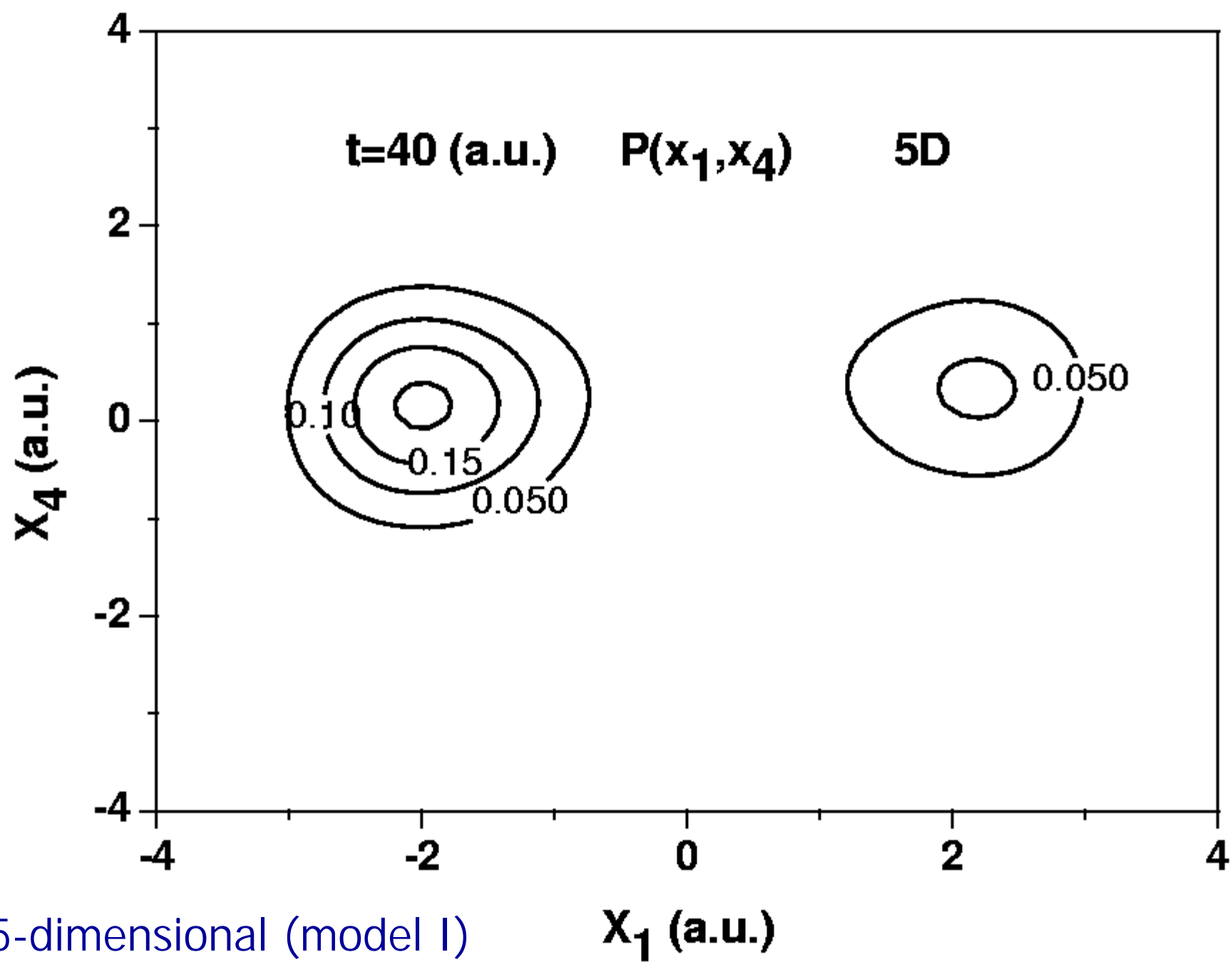


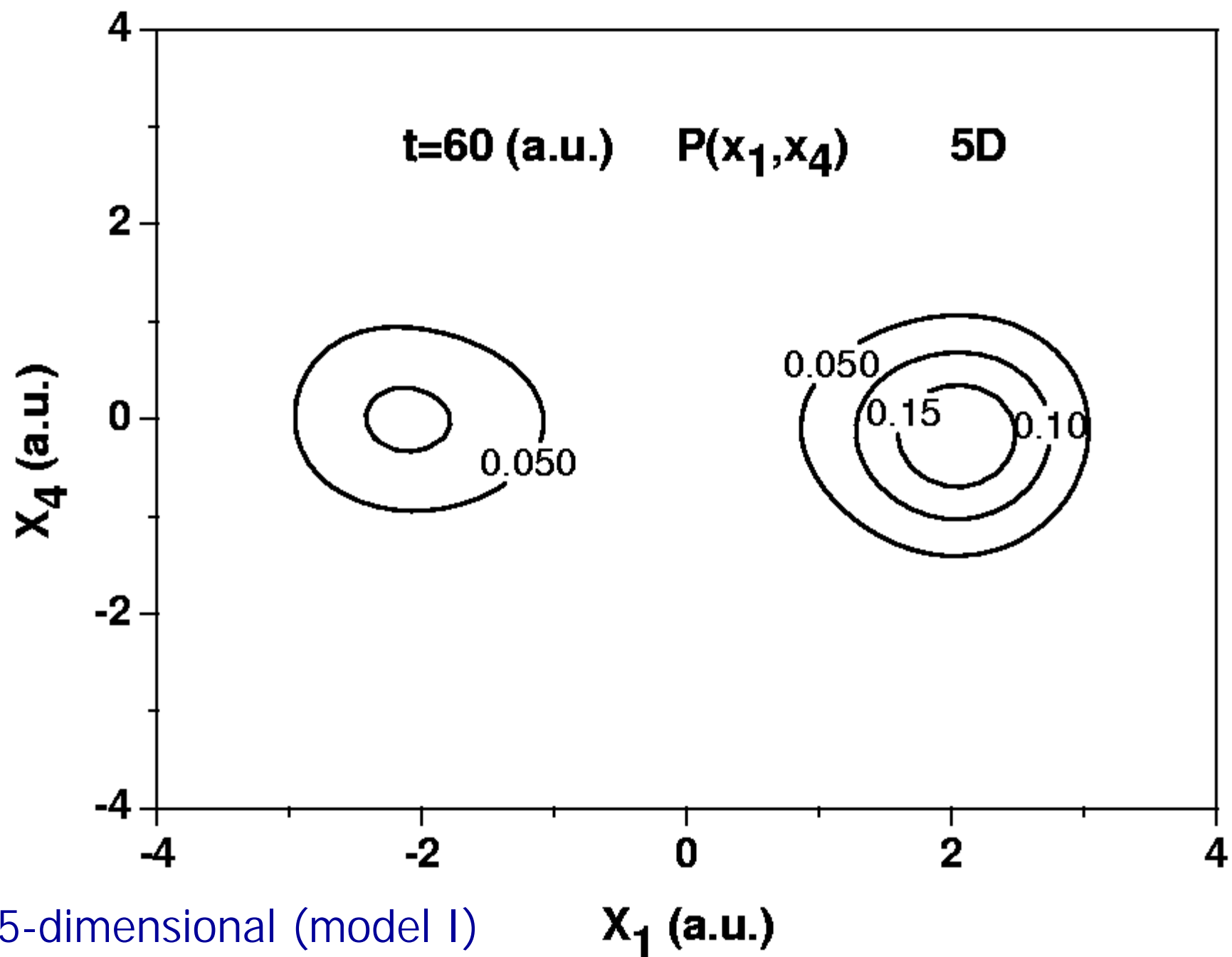


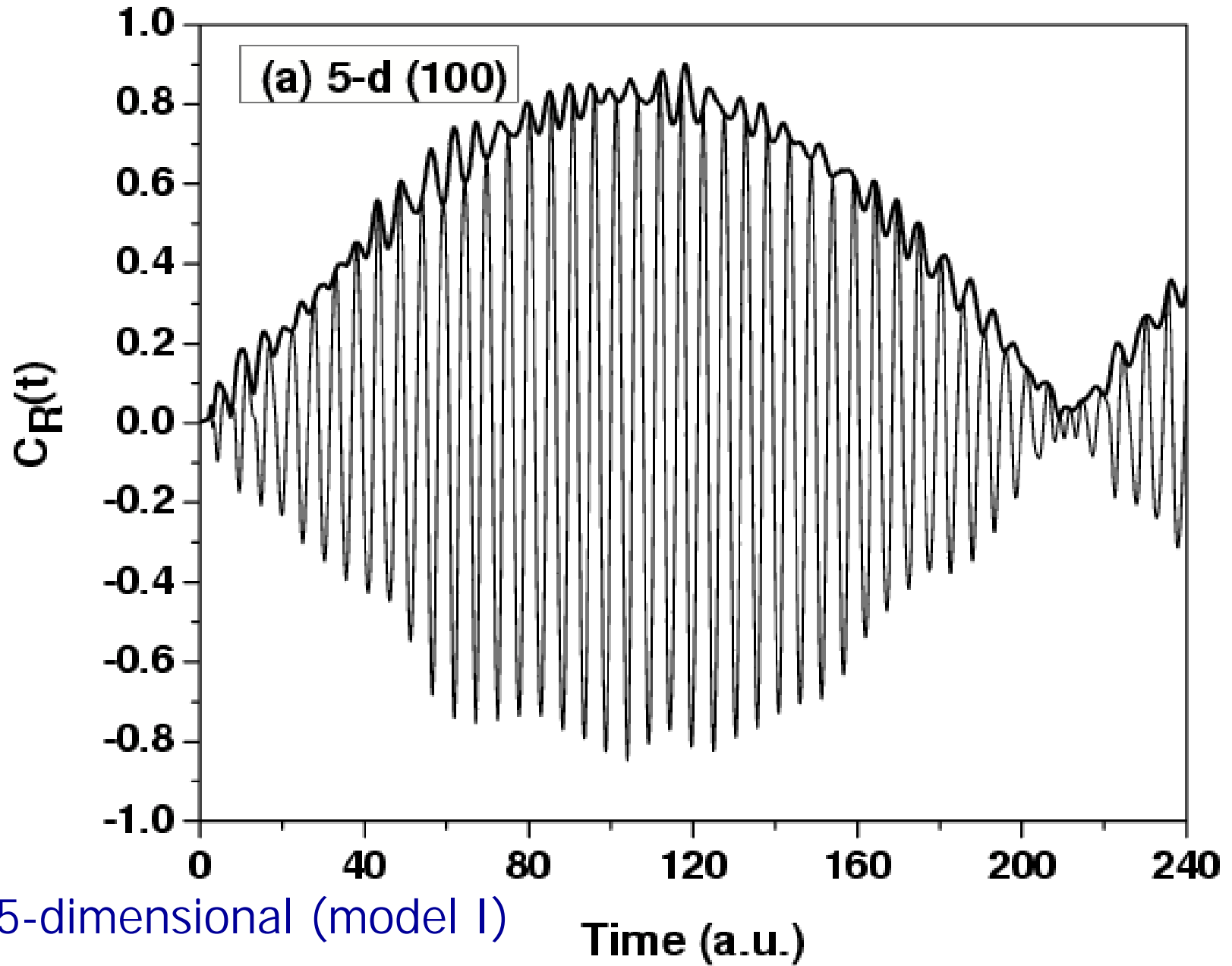


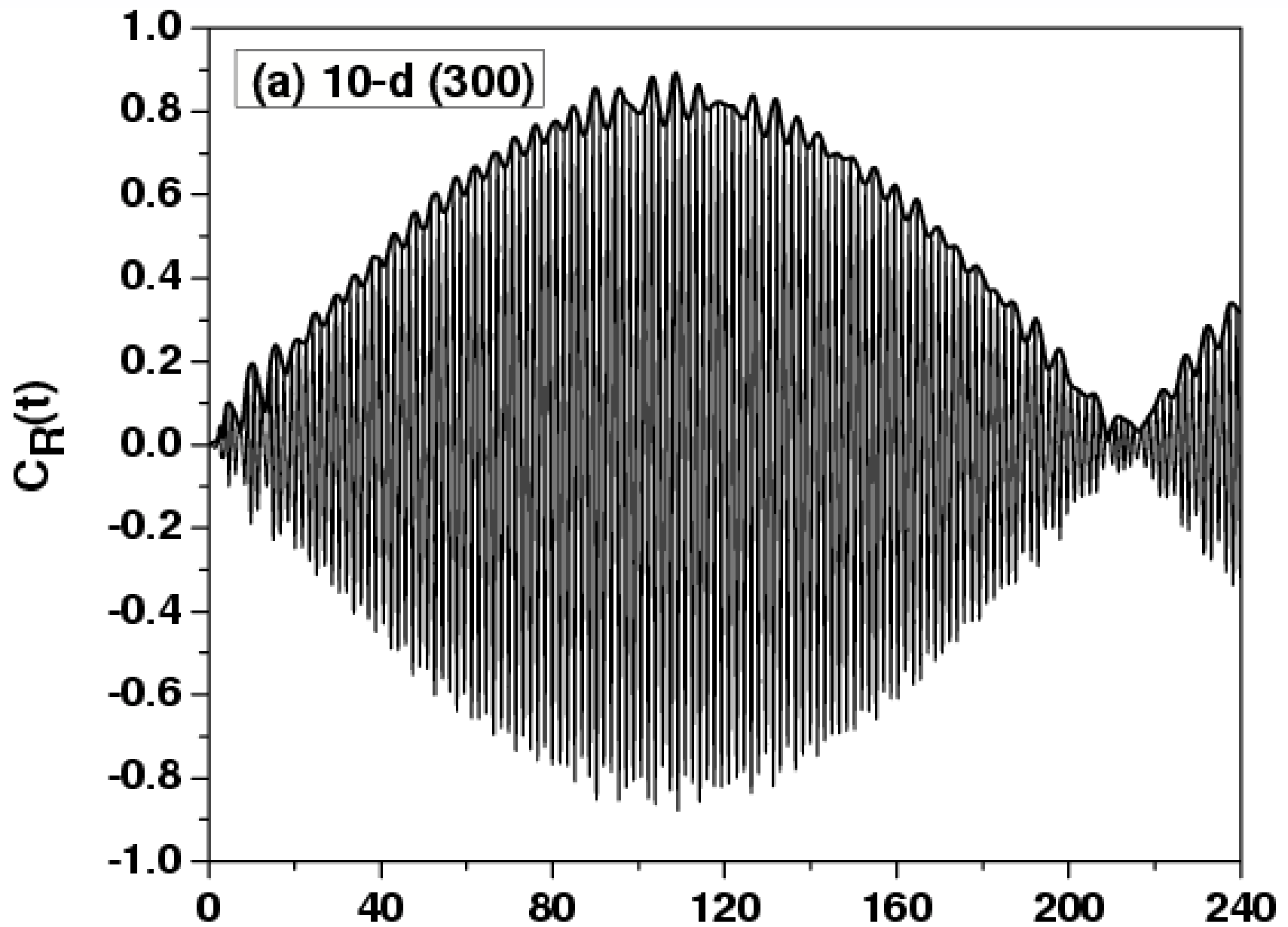












10-dimensional (model I) Time (a.u.)

Electron Tunneling in Multidimensional Systems

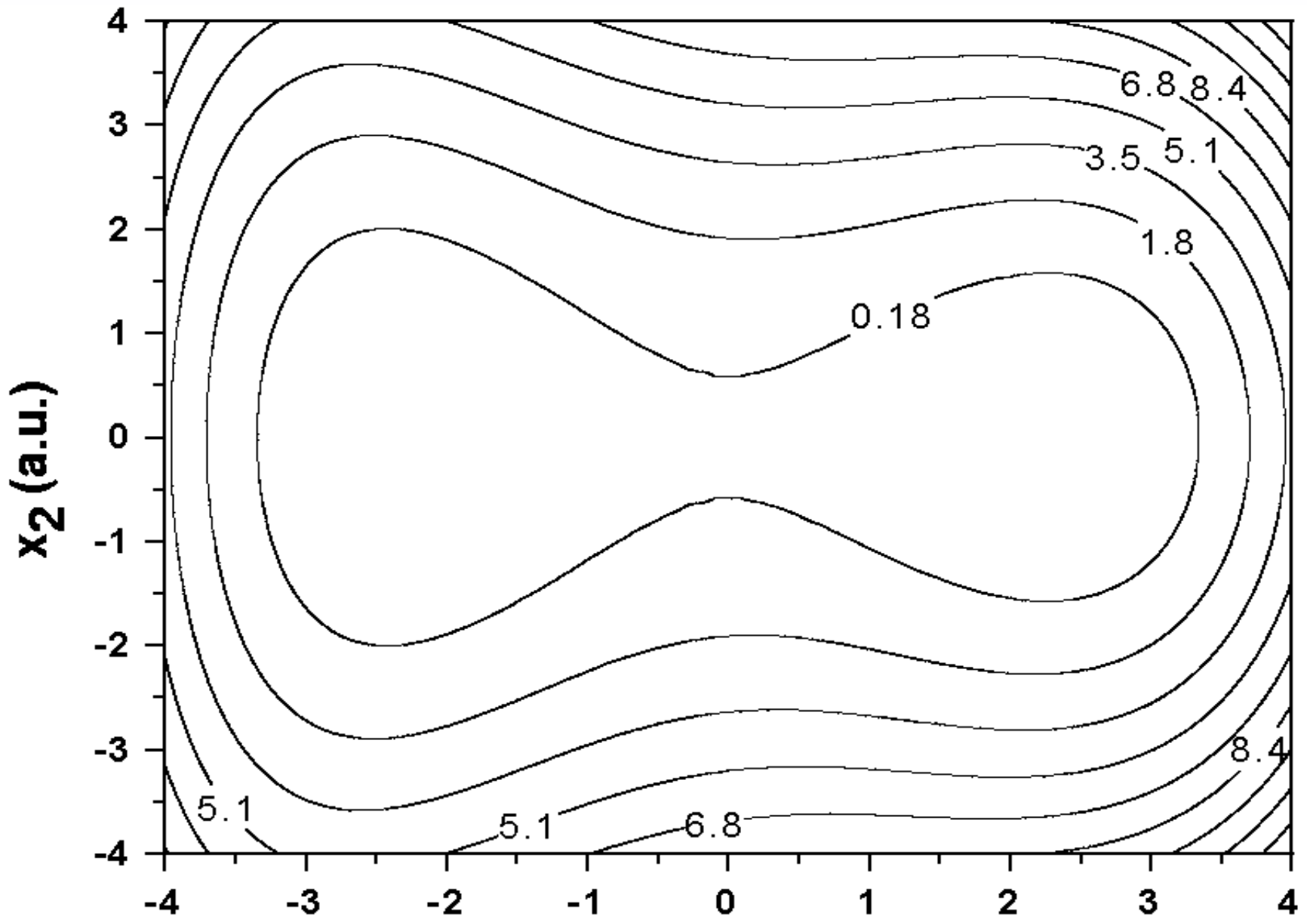
Model II

$$\hat{H} = \frac{\hat{p}_1^2}{2m_1} + V_1(\hat{x}_1) + \sum_{j=2}^N \left(\frac{\hat{p}_j^2}{2m_j} + \frac{1}{2}m_j\omega_j^2\hat{x}_j^2 + \frac{1}{2}c_j\hat{x}_1\hat{x}_j^2 \right),$$

where $m_j = 1.0$ a.u., $\omega_j = 1.0$ a.u. and $c_j = 0.1$ a.u. for $j = 1-N$ with $N = 1-20$.

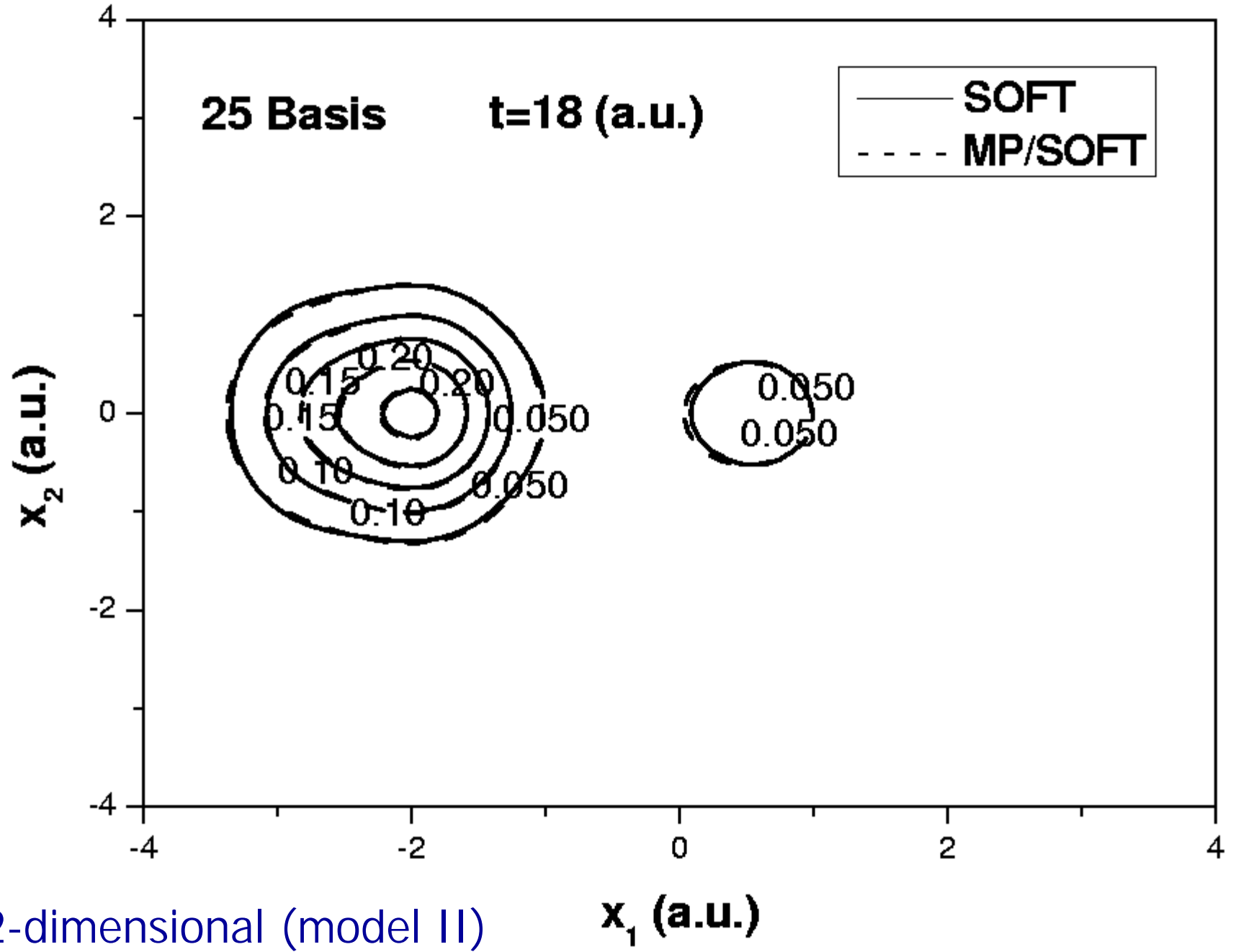
$$V_1(\hat{x}_1) = \frac{1}{16\eta}\hat{x}_1^4 - \frac{1}{2}\hat{x}_1^2,$$

with $\eta = 1.3544$.

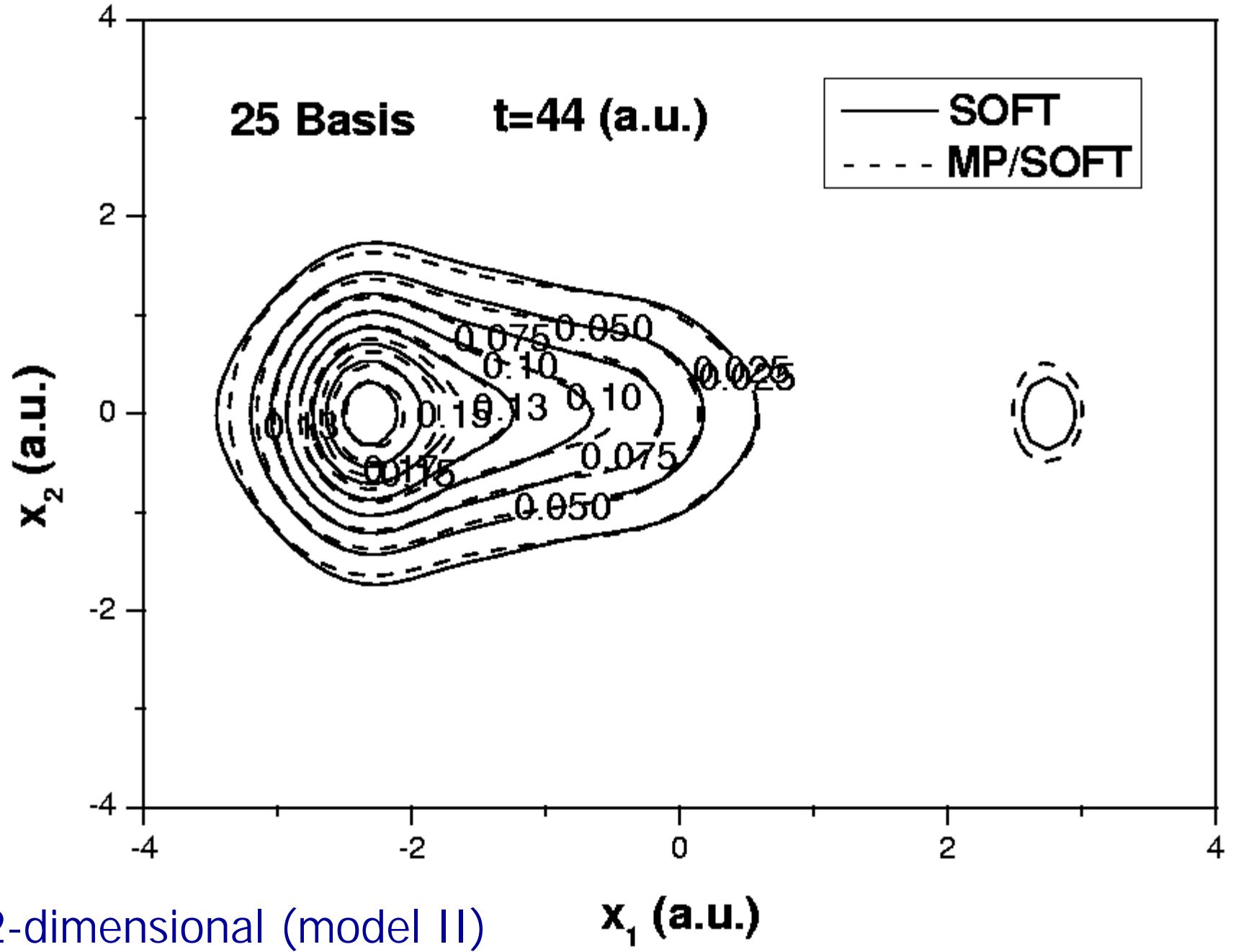


(2-dimension Model II)

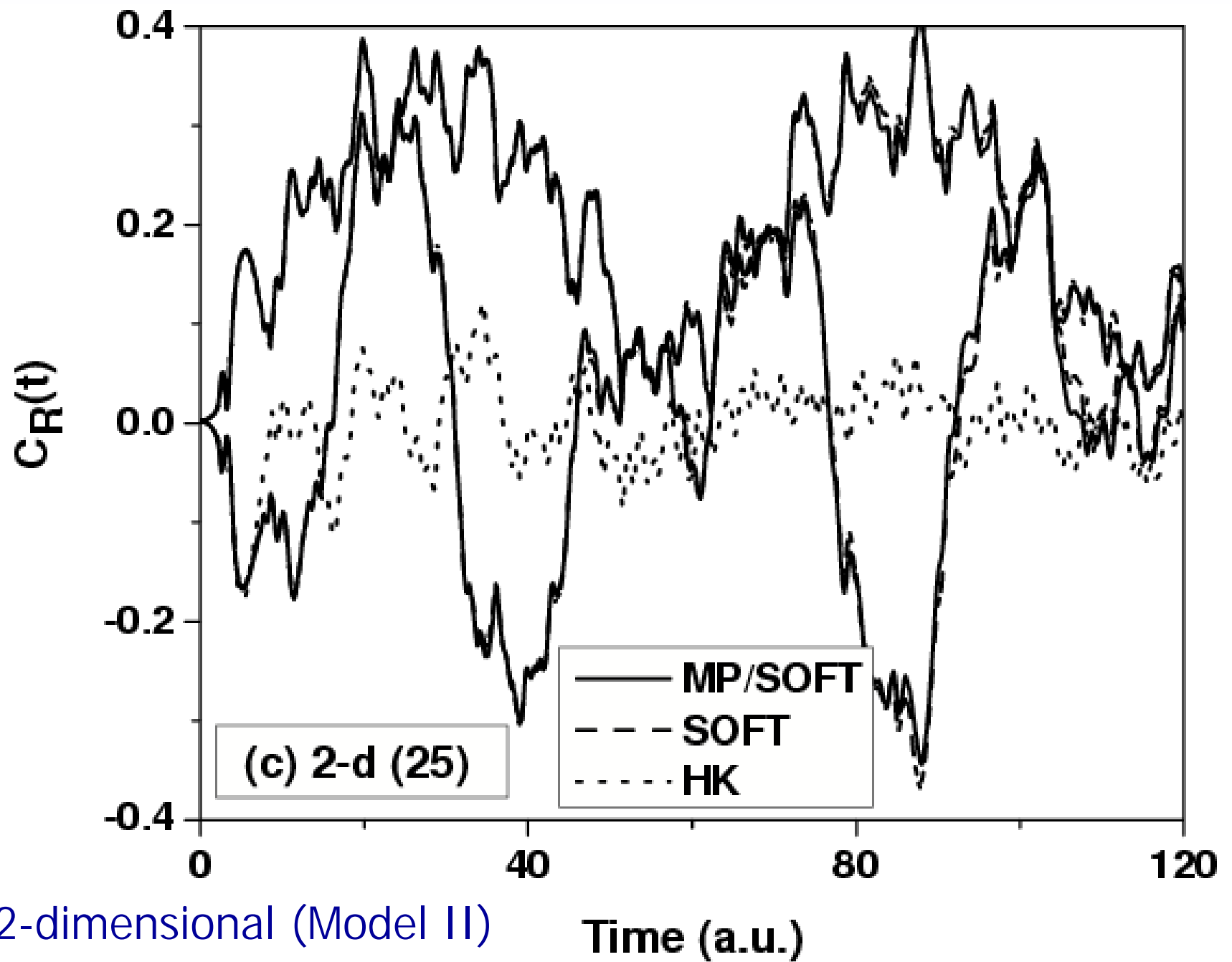
x_1 (a.u.)



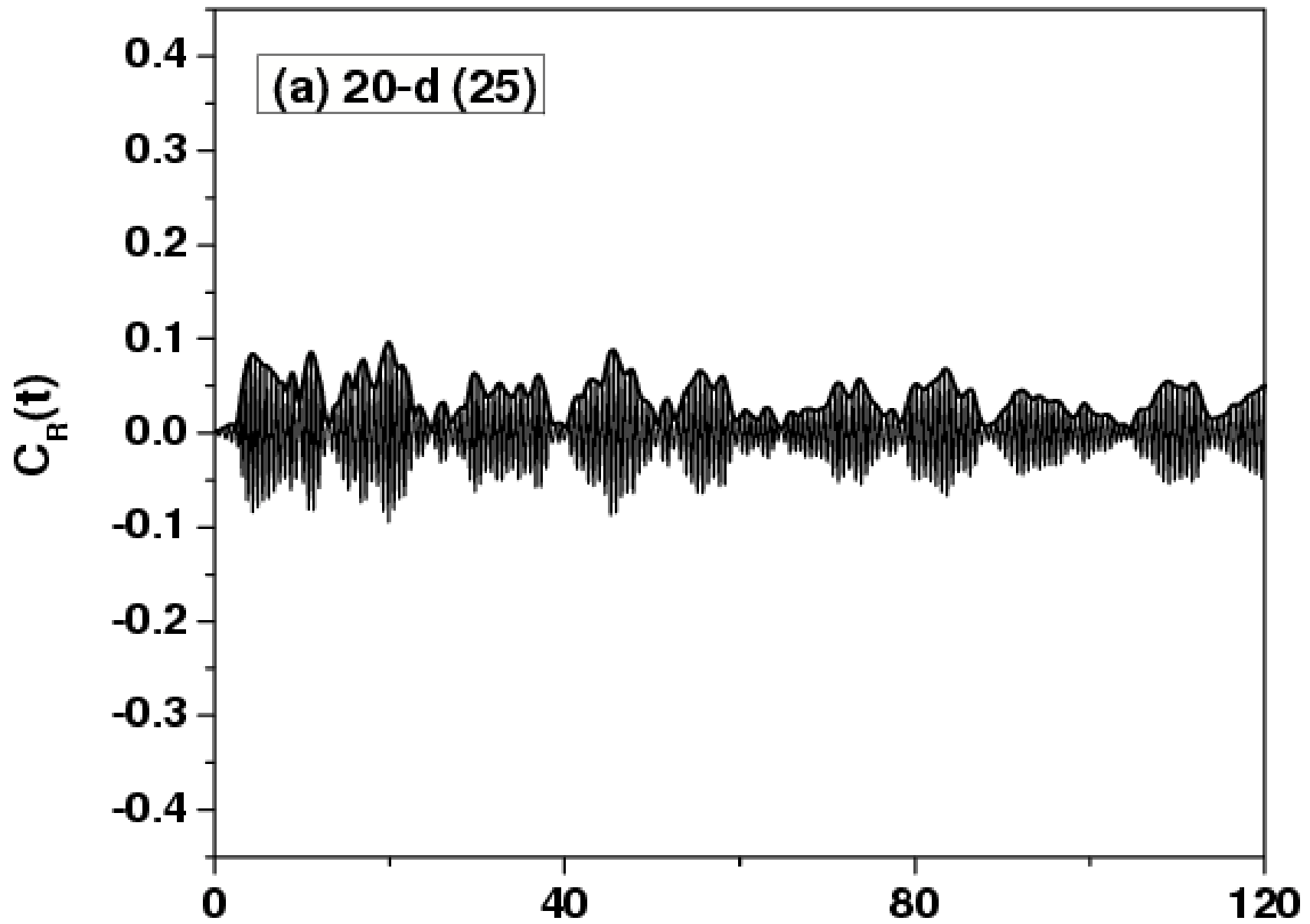
2-dimensional (model II)



2-dimensional (model II)

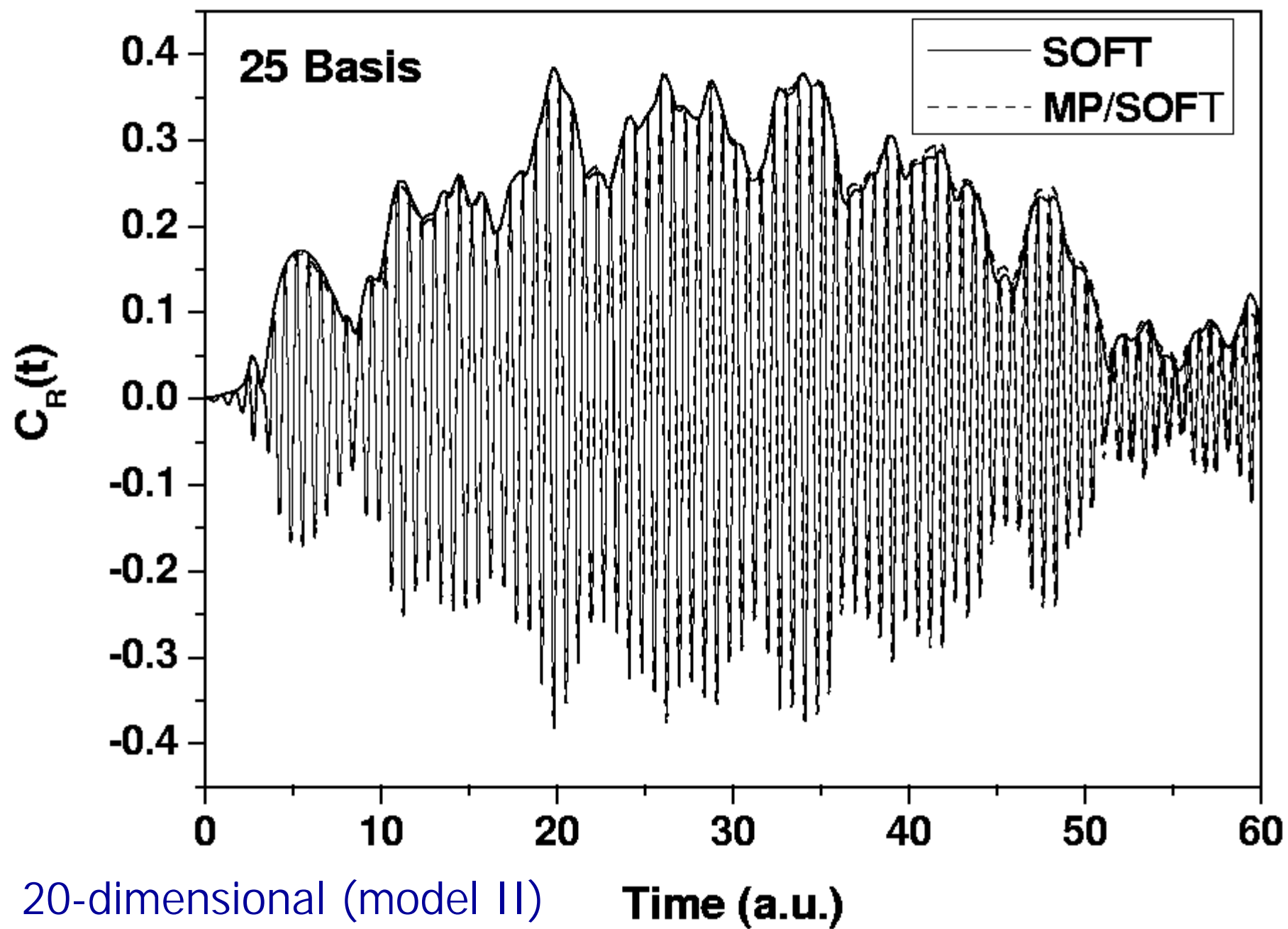


2-dimensional (Model II)



20-dimensional (Model II) Time (a.u.)

Benchmark calculation:



TS/SC-IVR Approach

Burant, J. and Batista, V.S. *J. Chem. Phys.* **116**, 2748 (2002).

Wu, Y. and Batista, V.S. *J. Phys. Chem. B* **106**, 8271 (2002).

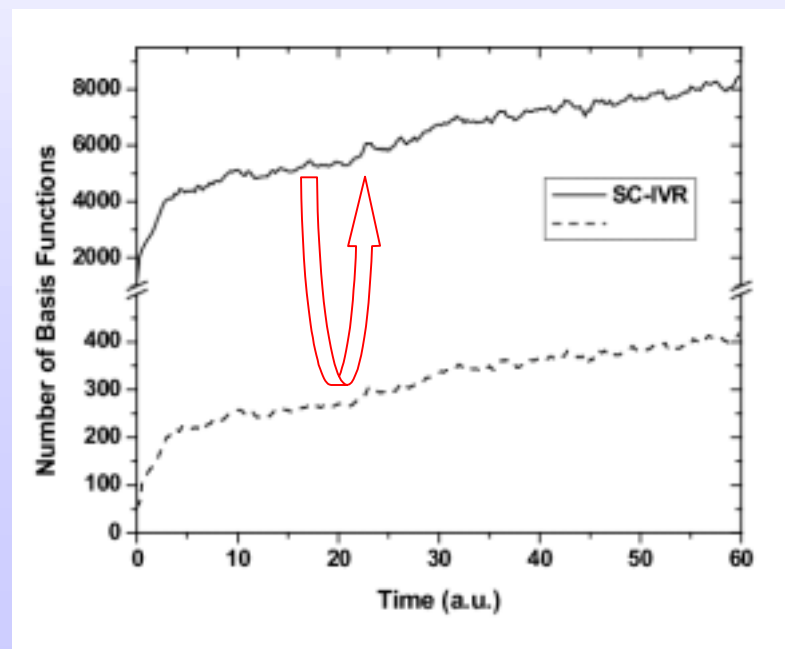
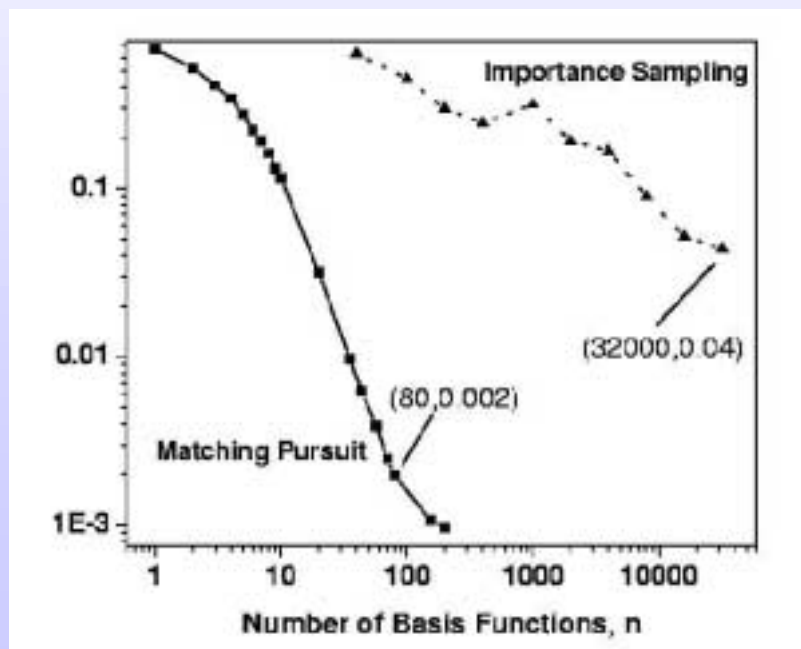
$$e^{-(i/\hbar)\hat{H}\tau} \approx (2\pi\hbar)^{-D} \int d\mathbf{p}_0 \int d\mathbf{q}_0 | \mathbf{p}_\tau \mathbf{q}_\tau \rangle C_\tau(\mathbf{p}_0 \mathbf{q}_0) e^{iS_\tau(\mathbf{p}_0, \mathbf{q}_0)/\hbar} \langle \mathbf{p}_0, \mathbf{q}_0 |,$$

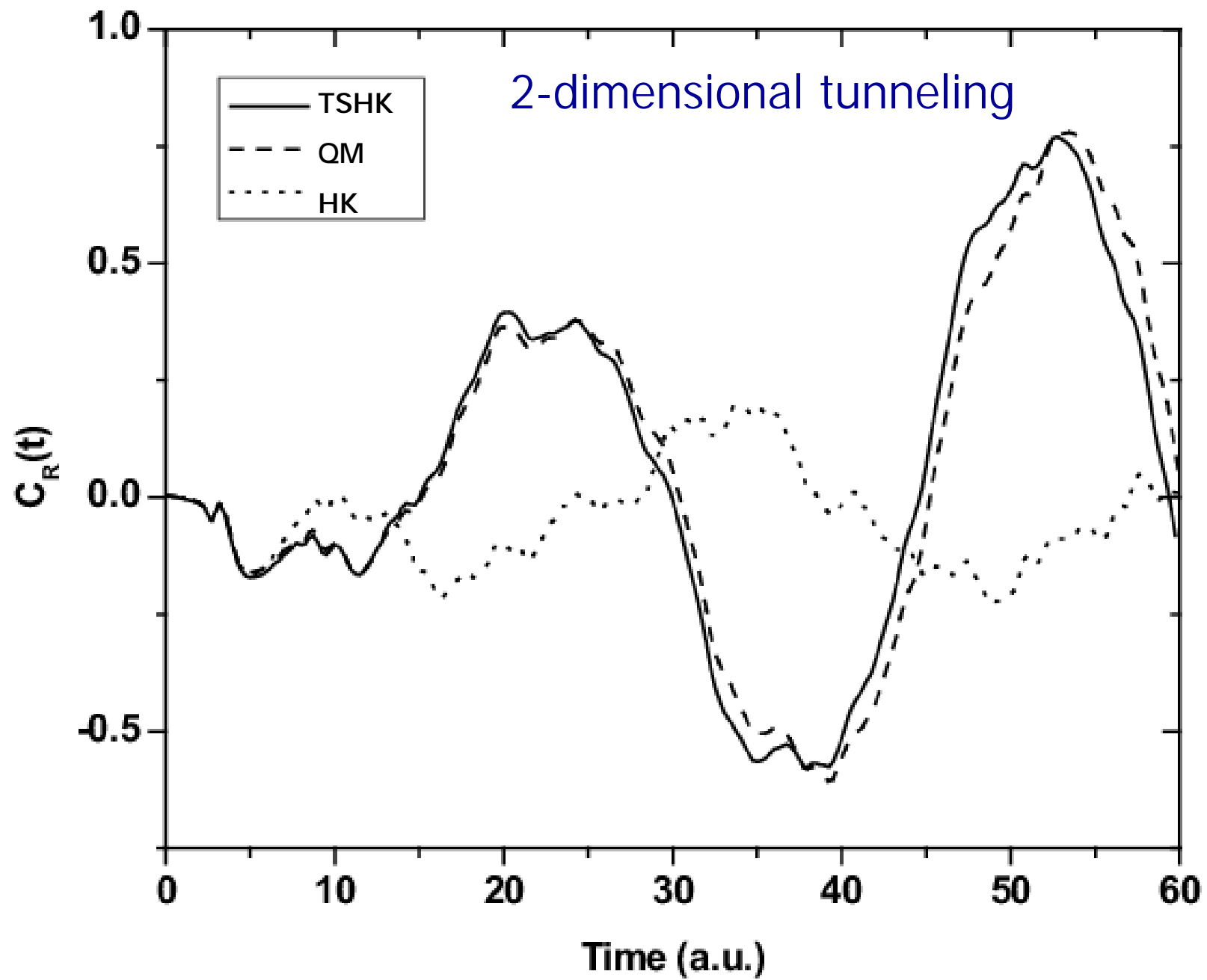
where D is the number of nuclear degrees of freedom and $| \mathbf{p}_\tau \mathbf{q}_\tau \rangle$ are the minimum uncertainty wavepackets, or coherent states (CS),

$$\langle \mathbf{x} | \mathbf{p}_\tau \mathbf{q}_\tau \rangle = \left(\frac{2\gamma}{\pi} \right)^{D/4} \exp \left[-\gamma(\mathbf{x} - \mathbf{q}_\tau)^2 + i\mathbf{p}_\tau(\mathbf{x} - \mathbf{q}_\tau)/\hbar \right],$$

The (TS) implementation avoids most of the difficulties of the standard SC-IVR, since the propagator is applied only for short time-slices while the semiclassical approximation is still accurate and efficient. However, the method introduces a new challenge: the reinitialization of the time-evolved wavefunction after each propagation time-slice.

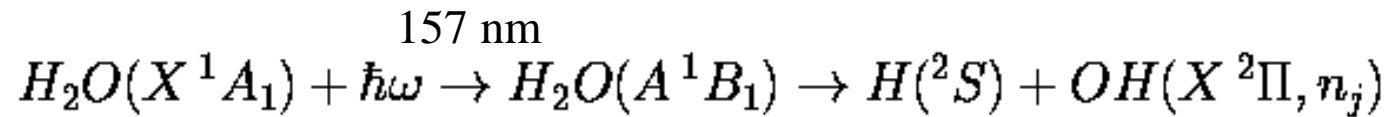
In order to optimize the efficiency of the re-expansion procedure, the time-evolved wavefunction is represented ("compressed") at the end of each propagation time-slice according to a matching-pursuit coherent-state expansion.





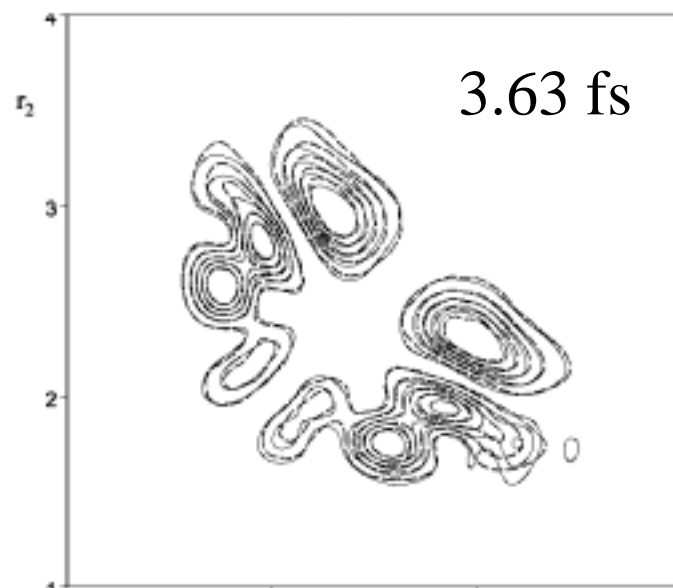
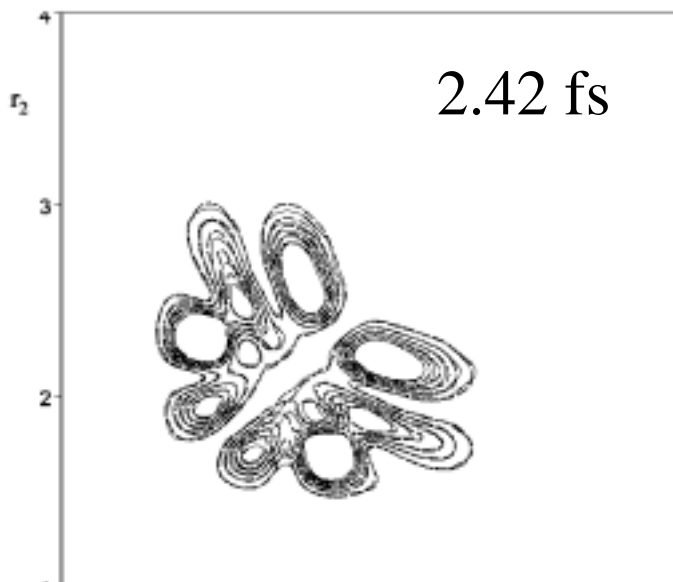
TS/SC-IVR Approach

Photodissociation of H₂O in the A ¹B₁ Band

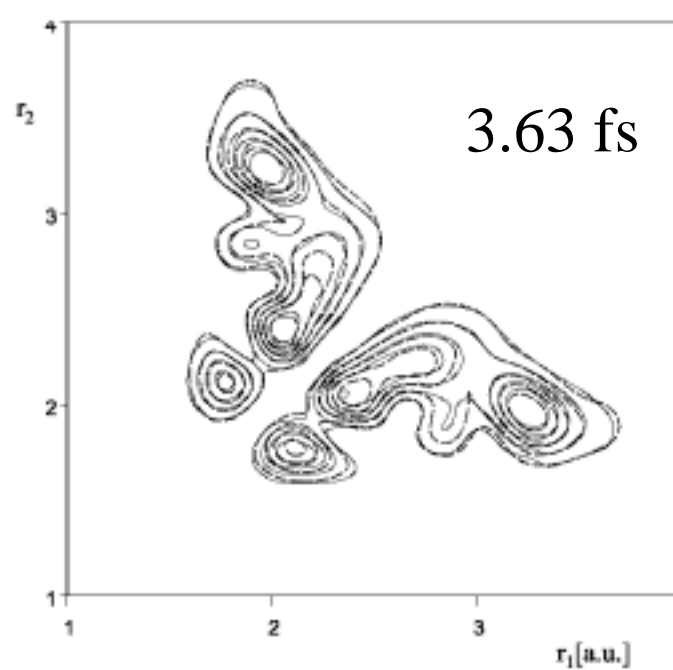
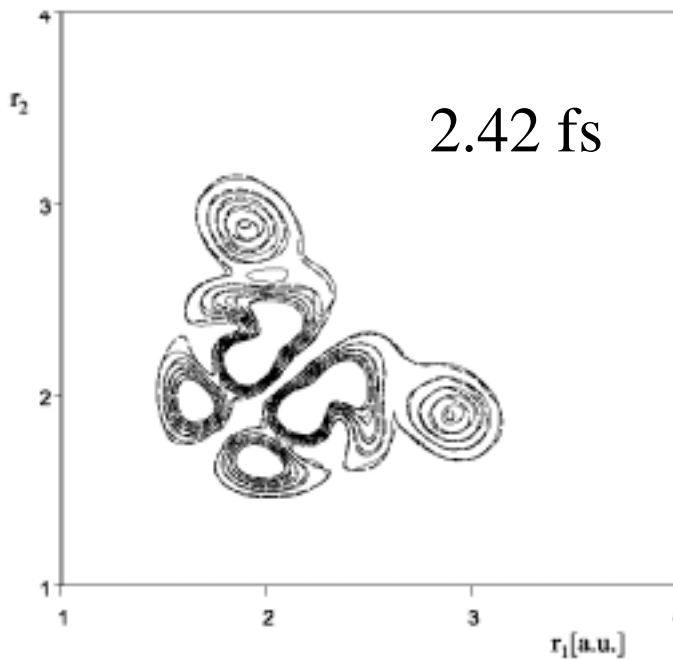


Instantaneous Time-Dependent Wavepackets

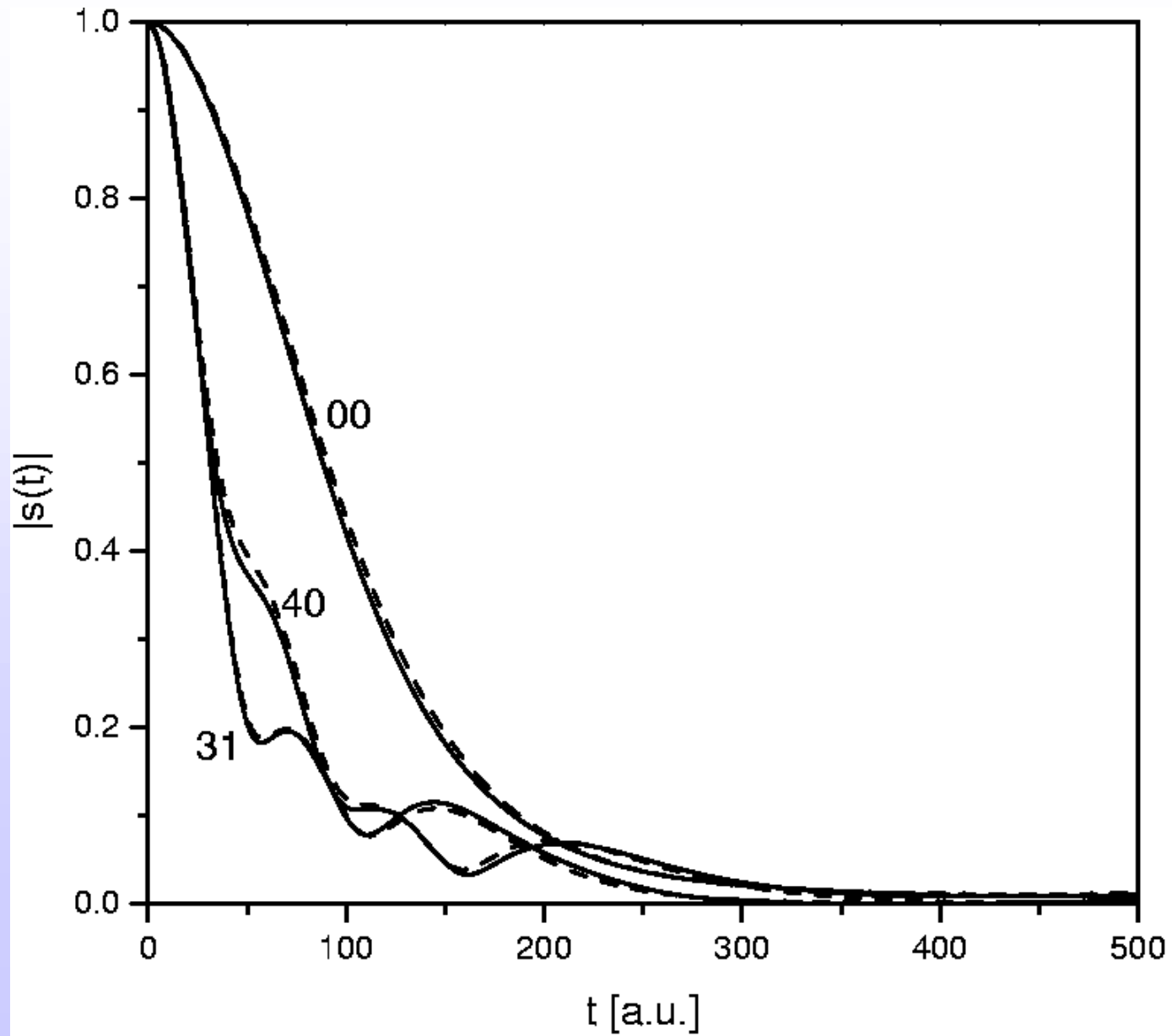
$|31\rangle$



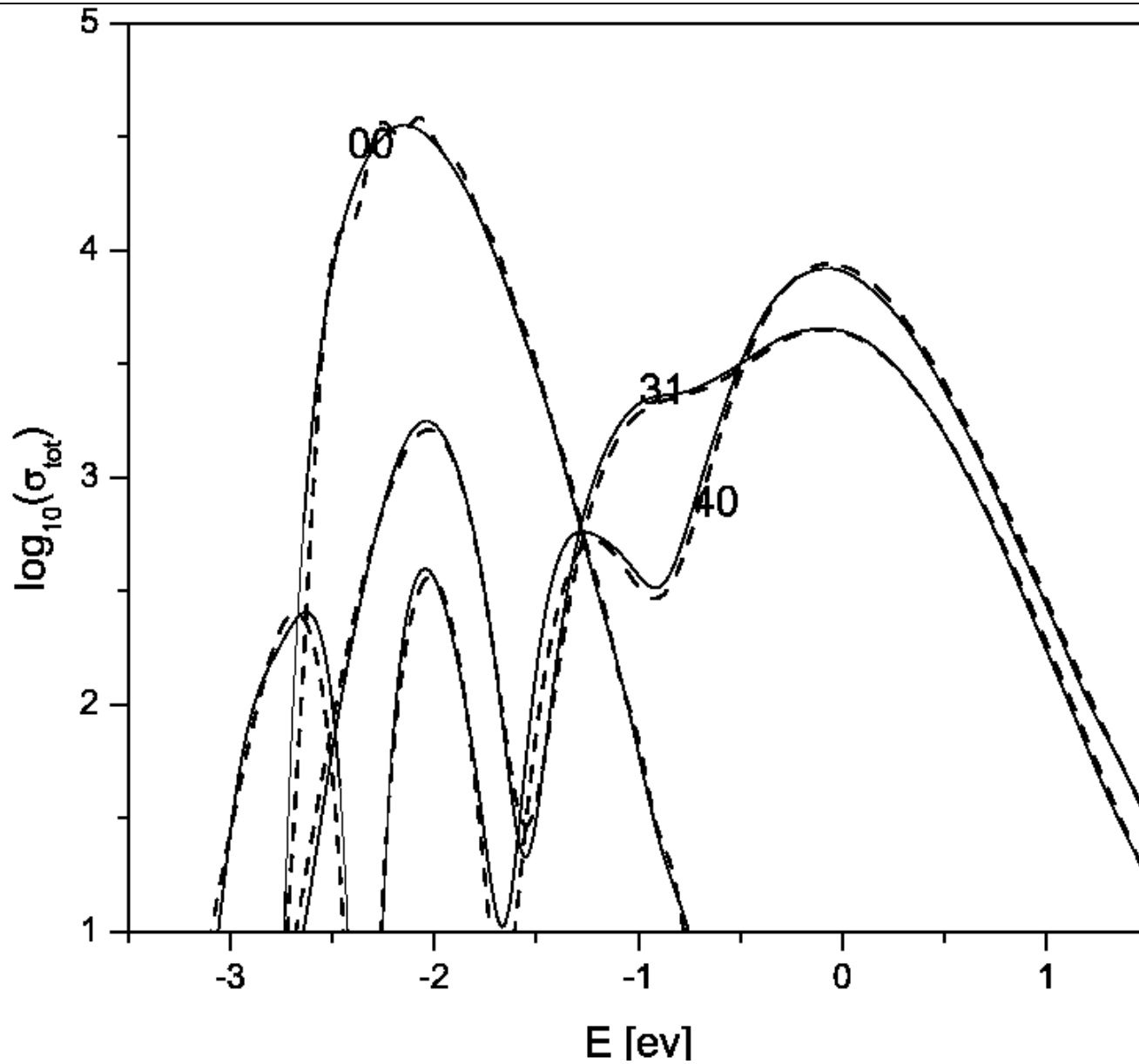
$|40\rangle$



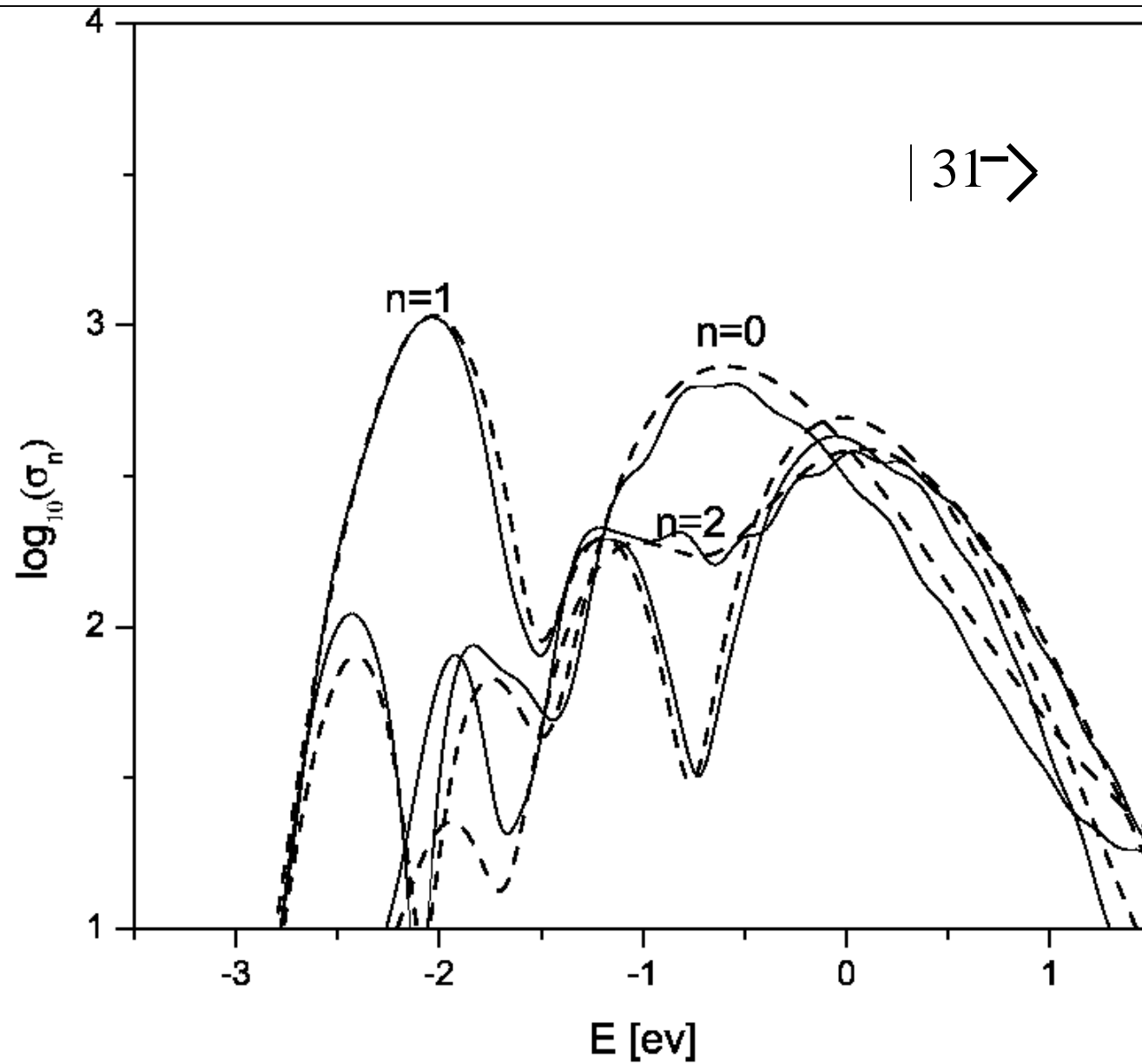
Survival Amplitudes



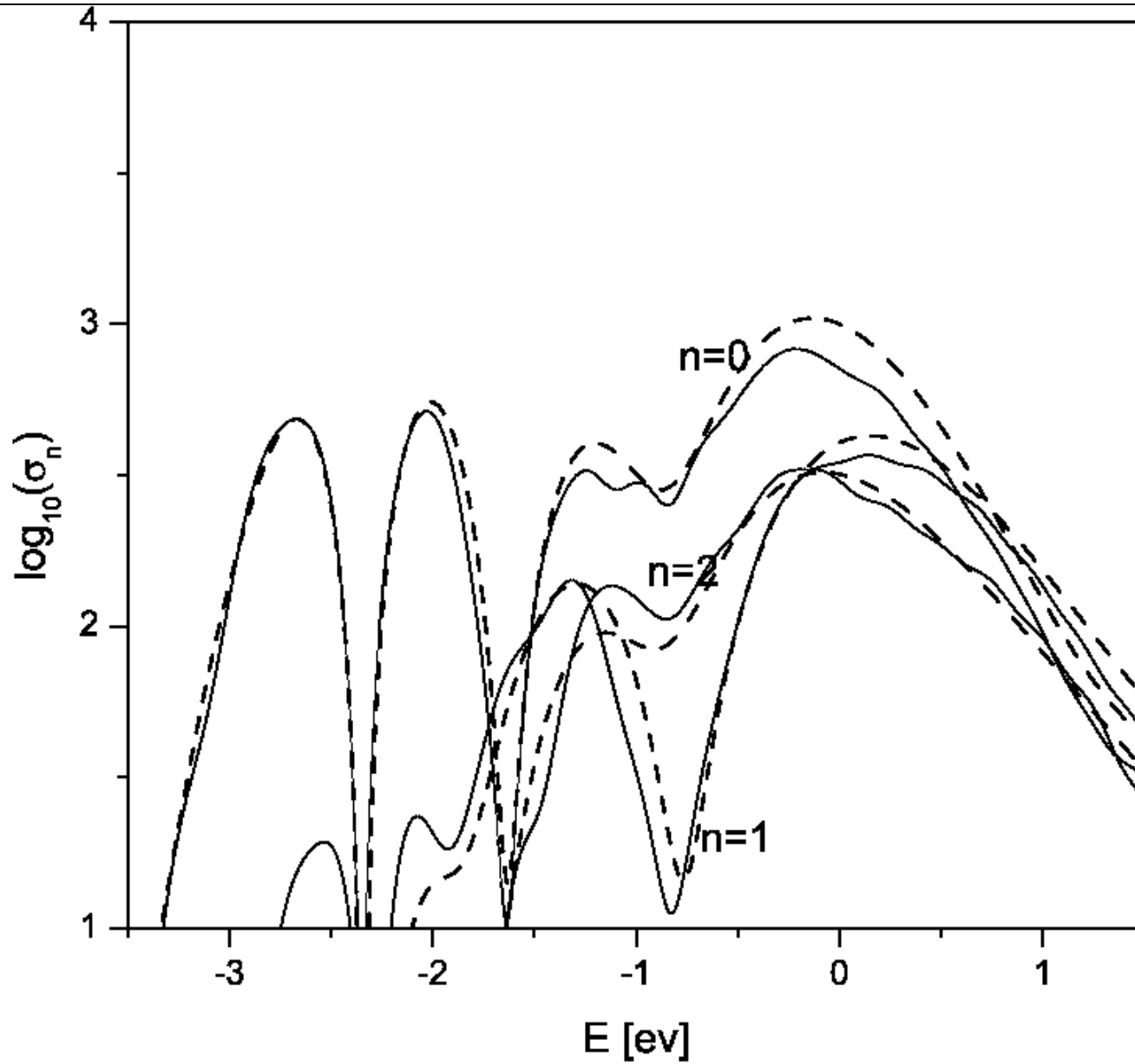
Total Photodissociation Cross Sections



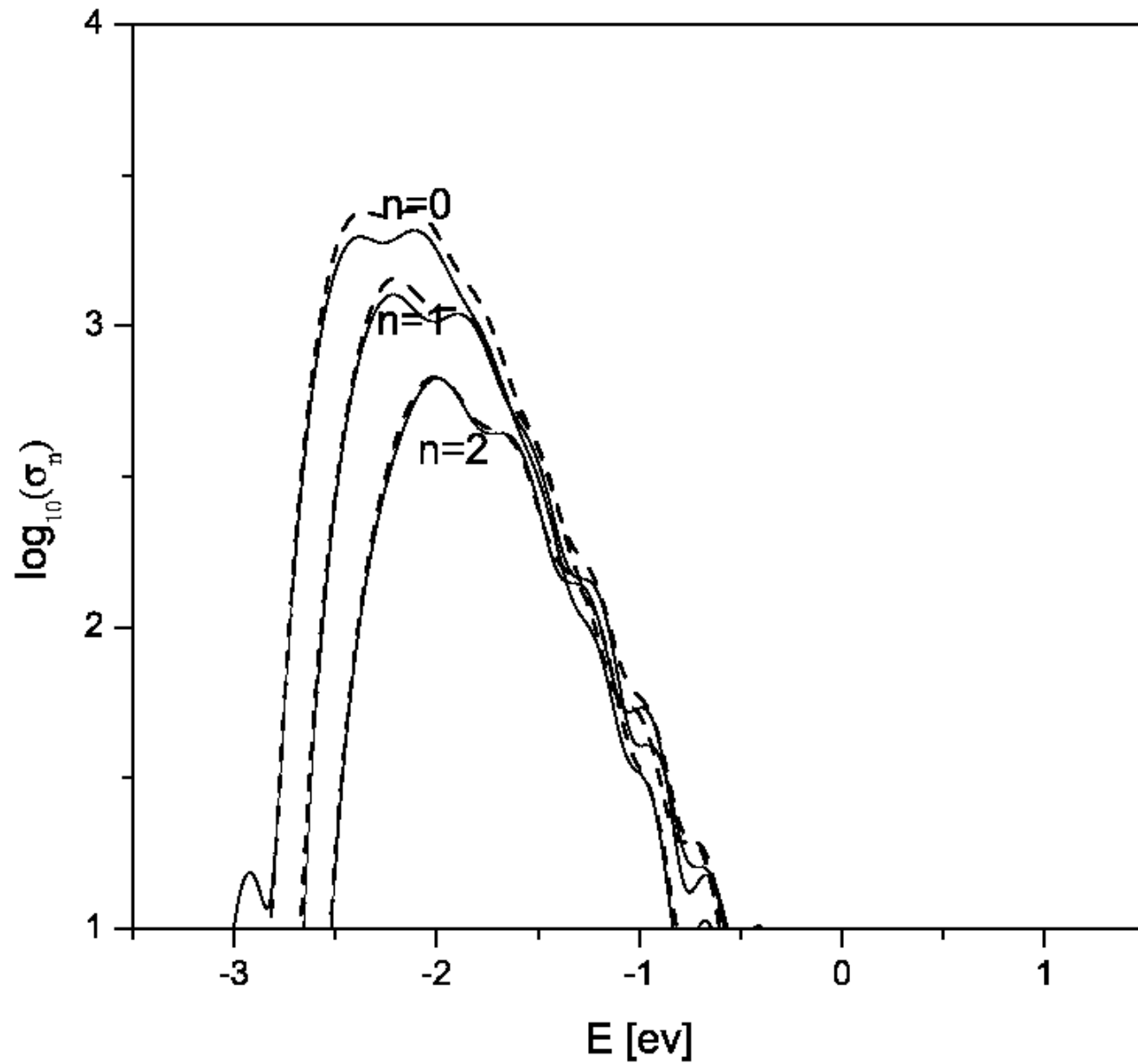
Partial Photodissociation Cross Sections



Partial Photodissociation Cross Sections



Partial Photodissociation Cross Sections



Conclusions

- We have introduced the MP/SOFT method for time-sliced simulations of quantum processes in systems with many degrees of freedom. The MP/SOFT method generalizes the grid-based SOFT approach to non-orthogonal and dynamically adaptive coherent-state representations generated according to the matching-pursuit algorithm. The accuracy and efficiency of the resulting method were demonstrated in simulations of deep-tunneling quantum dynamics for systems with up to 20 coupled degrees of freedom.
- Work in progress involves simulations of excited-state intramolecular proton transfer in 2,2'-hydroxyphenyl-oxazole as well as calculations of the equilibrium density matrix (equilibrium properties of quantum systems).
- We have also introduced the TS/SC-IVR approach, a method that concatenates finite-time propagators and computes real-time path integrals based on the HK SC-IVR. We have shown that the approach significantly improves not only the accuracy of simulations of deep-tunneling quantum dynamics based on the HK SC-IVR but also the accuracy of computations of photo-dissociation cross sections of vibrationally hot molecules (sensitive to subtle interference effects).

Acknowledgment

- NSF Career Award
- ACS Petroleum Research Funds (Type G)
- Research Corporation, Innovation Award
- Hellman Family Fellowship
- Anderson Fellowship
- Yale University, Start-Up Package